

AN INVESTIGATION OF THE CRUDE OIL IN THE SPIVEY-GRABS FIELD OF SOUTH-
CENTRAL KANSAS: AN INSIGHT INTO OIL TYPE AND ORIGIN

by

BRIANNA KWASNY

B.S., University of Oklahoma, 2013

A THESIS

submitted in partial fulfillment of the requirements for the degree

MASTER OF SCIENCE

Department of Geology
College of Arts and Science

KANSAS STATE UNIVERSITY
Manhattan, Kansas

2015

Approved by:

Major Professor
Matthew Totten

Copyright

BRIANNA KWASNY

2015

Abstract

The most common practice of typing crude oils utilizes biomarkers to gain insight on the history of the oil. This practice only considers the organic chemistry of the oil, and does not consider the trace element concentrations within the oil. Rare earth element and other trace element concentrations in crude oil might provide further insight into the oil's source and origin. This study analyzed REE and other trace metal concentrations of crude oil in the Spivey-Grabs field of south-central Kansas through analysis by ICP-MS and ICP-AES that, coupled with visual physical characteristics of oil and FT-IR analysis, could explain the reported "compartmentalization" of the field and provide insight on the origin of the oils. Analysis of physical characteristics of the crude oils suggested the presence of two types of oil, of differing viscosities, in the field. FT-IR confirmed the presence of these two oil types based on functional groups present in the oils. The existence of a high viscosity oil could potentially explain the compartmentalization behavior in the field.

PAAS-normalized REE distribution patterns showed a general LREE enrichment, a positive cerium and negative europium anomaly, and a MREE and HREE depletion, but higher viscosity oils showed additional MREE and HREE enrichment. K/Rb values ranged from 2,864 to 44,118, with oils from mixed-viscosity wells having lower ratios overall. K/Rb values of Spivey-Grabs crude oils more closely resembled those of the Lansing-Kansas City formation than the K/Rb values of the Woodford shale and Mississippian formation of the Anadarko basin. Comparing the rare earth element distribution patterns and K/Rb values from this study to those of the Woodford shale suggests the Spivey-Grabs oil originated from a local source and not from the Woodford shale.

Table of Contents

List of Figures	vi
List of Tables	ix
Acknowledgements	x
Chapter 1 - Introduction	1
Chapter 2 - Background	5
2.1 Geologic Setting	5
2.1.1 Regional Environment of Deposition	5
2.1.2 Regional Stratigraphy	7
2.1.3 The Spivey-Grabs Field	16
2.2 Geochemistry of Crude Oils	19
Chapter 3 – Geochemistry of Spivey-Grabs Oil	23
Chapter 4 - Methods	25
4.1 Field Methods	25
4.1.1 Study Area and Sample Locations	25
4.1.2 Sample Collection	27
4.2 Analytical Methods	28
4.2.1 Methodology for Infrared Absorption Spectral Analysis	28
4.2.2 Methodology for REE and Trace Metal Analysis	28
4.2.3 Potential Sources for Analytical Error	32
Chapter 5 - Results	34
5.1 Physical Characteristics of Crude Oils	34
5.2 Infrared Spectroscopy Results	35
5.3 REE and Trace Metal Concentrations in Crude Oils	37
Chapter 6 - Discussion	40
6.1 Two Types of Oil in the Spivey-Grabs Field	40
6.1.1 Physical Characteristics of Oil	40
6.1.2 Distinction of Oils by Functional Groups	41
6.2 Field Compartmentalization Due to Two Different Oils Within the Field	44
6.3 Distribution of Rare Earth Elements in Spivey-Grabs Oil	44

6.3.1 REE Anomalies and Similar Distribution Patterns of Spivey-Grabs Crude Oil.....	45
6.3.2 REE Distribution Patterns of Spivey-Grabs Crude Oil Compared to Other Oils	51
6.4 K/Rb Indicate Two Oil Types and Local Source.....	53
6.4.1 K/Rb Values of the Spivey Grabs Field Oil.....	53
6.4.2 K/Rb Values of Spivey Grabs Oil Compared to Other Oils	55
6.5 Biomarker Maturation Groups Compared to Inorganic Constituents.....	57
6.6 Implications of REE Distribution Patterns and K/Rb Comparisons.....	58
Chapter 7 - Conclusions.....	60
References.....	62
Appendix A – Rare Earth Elements (REE).....	66
Appendix B – REE Distribution Patterns	69
Appendix C – Fourier Transform Infrared Spectroscopy (FT-IR)	73
Appendix D – Sample Dilutions	75

List of Figures

Figure 1 Locations of chert hydrocarbon reservoirs across the United States and Canada (Rogers and Longman, 2001)	3
Figure 2 Arcuate fairway of productive Mississippian chat reservoirs shown in relation to regional structures across Kansas (Montgomery et al., 1998)	4
Figure 3 Location of Spivey-Grabs Field in relation to other major chat reservoirs in south-central Kansas. Modified from Montgomery et al. (1998)	4
Figure 4 Paleogeographic map showing shelf locations during Mississippiantimes (Watney et al., 2001)	6
Figure 5 Paleogeographic map showing the location of Kansas and its relation to the equator during Mississippian times (Mazzullo et al., 2009).	6
Figure 6 Map of North America showing the location of Kansas in relation to the Canadaian shield and the extension of the shield, the Central Stable Region (Harris and Larsh 1976-1979)	8
Figure 7 Subsurface extent of Mississippian rocks in Kansas in gray (Merriam, 1963)	9
Figure 8 Structural features in Kansas showing uplift features where Mississippian rocks were eroded (Merriam, 1963)	10
Figure 9 Stratigraphic column depicting Mississippian nomenclature used in Kansas (Evans and Newell, 2013).....	11
Figure 10 Stratigraphic column depicting Mississippian rocks in Kansas with most recent placement of the Cowley Formation shown (Mazzullo et al., 2009).....	14
Figure 11 Subsurface extent of the Cowley Formation in orange in relation to regional post-Mississippian - pre-Desmoinesian tectonic elements with some of the larger Mississippian chert and/or spiculite oil and gas fields in green (Mazzullo et al., 2009)	15
Figure 12 Mississippian oil and and gas production locations in relation to major subsurface structural features in Kansas (Evans and Newell, 2013)	17
Figure 13 Relative distribution patterns of REEs in crude oil from the Lansing-Kansas City formation. Grouped samples show four distinct zones with similar distribution patterns. Zones of production are highlighted with correlating colors. Modified from McIntire 2014	20

Figure 14 Lansing-Kansas City crude oil K/Rb ratios from McIntire 2014	21
Figure 15 REE relative distribution patterns of Anadarko basin oils from Ramirez-Caro 2013. Top) Mississippian oil samples; Bottom) Devonian Woodford samples	22
Figure 16 Biomarker Maturity Index with samples displayed from Evans (2011) showing the two maturity indices present in the Spivey-Grabs Field	24
Figure 17 Map of Kansas with sample location in red. Modified from Merriam, 1963	25
Figure 18 Map showing locations where samples were collected within the Spivey-Grabs Field	26
Figure 19 Oil separation flowchart showing strategies of methods. Modified from Rameriz-Caro (2013)	32
Figure 20 Oil Samples with both heavy and light oil. A) is sample number BK-14-03 and B) is sample number BK-14-09	34
Figure 21 FT-IR spectra for each of the samples analyzed	36
Figure 22 FT-IR spectra of crude oil samples from the Spivey-Grabs field showing two distinct groups. Top) all light oil spectra; bottom) all heavy oil spectra	41
Figure 23 FT-IR spectra of light and heavy oils highlighting peaks that are present in the heavy oil but not in the light oil	42
Figure 24 Graph showing the first derivatives of both BK-14-09A and BK-14-09B, as well as the difference in their first derivatives. This shows that there is a peak shift located between 2800 cm^{-1} and 3000 cm^{-1}	43
Figure 25 PAAS-normalized abundance diagram displaying the relative distribution patterns of all oil samples from the Spivey-Grabs Field	45
Figure 26 REE distribution patterns of organic portion of the Chattanooga shale showing negative Ce anomalies and positive Eu anomalies (Wall, 2015)	47
Figure 27 Relative distribution patterns of REEs grouped by similar distribution patterns	48
Figure 28 Relative distribution pattern of REEs in BK-14-03A and BK-14-07 grouped by similar distribution patterns	49
Figure 29 Relative distribution pattern of REEs in BK-14-08	49
Figure 30 Relative distribution patterns of REE in crude oils samples from the Spivey-Grabs field and McIntire's (2014) Lansing-Kansas City samples grouped by similar distribution patterns. All seven samples have an enrichment of LREE and depletion of MREE and HREE	52

Figure 31 Chart showing the K/Rb values of crude oils from the Spivey-Grabs field compared to the average K/Rb value of silicate minerals/clays	54
Figure 32 High, low, and average K/Rb ratios from crude oils from: Top) the Spivey-Grabs field and Lansing-Kansas City formation; Bottom) the Spivey Grabs field and the Mississippian and Woodford oils from the Anadarko basin. Compared on a logarithmic scale.	56
Figure A.1 Rare earth elements (lanthanide series) in the Periodic Table of Elements	66
Figure A.2 Graph depicting lanthanide contraction and REE relative distribution pattern group	68
Figure B.1 REE distribution pattern of BK-14-01	69
Figure B.2 REE distribution pattern of BK-14-03A	69
Figure B.3 REE distribution pattern of BK-14-05	70
Figure B.4 REE distribution pattern of BK-14-06A	70
Figure B.5 REE distribution pattern of BK-14-07	71
Figure B.6 REE distribution pattern of BK-14-08	71
Figure B.7 REE distribution pattern of BK-14-09A	72

List of Tables

Table 1 Well locations and corresponding samples names. Sample locations also in Evans (2011) are highlighted in blue.....	27
Table 2 Physical characteristics of oils from the Spivey-Grabs field. Samples also in Evans (2011) are highlighted in blue.....	35
Table 3 REE and trace element analytical results for oil from the Spivey-Grabs Field. Concentrations in ppb. REEs are highlighted by red box. Samples also in Evans (2011) are highlighted in blue	38
Table 4 Trace element analytical results for oil from the Spivey-Grabs Field. Concentrations of Si to P in ppm. Concentrations of Sr to Cu in ppb. Samples also in Evans (2011) are highlighted in blue	39
Table 5 Extent of cerium anomaly in each sample. Samples also in Evans (2011) are highlighted in blue.....	46
Table 6 Inorganic constituent analyses compared to biomarker maturation indices from Evans (2011). Blue) less mature oil group; red) mature oil group; white) not analyzed in Evans' study	58
Table A.1 Atomic number and ionic radii for the REE	67
Table C.1 Table showing the assignment of the primary infrared bands/peaks to functional groups	74
Table D.1 Sample dilutions that occurred during preparation of the samples for analysis	75

Acknowledgements

I would like to thank my graduate advisors, Dr. Matthew Totten and Dr. Sambhudas Chaudhuri for all of the meetings, call, texts and emails we shared over the course of my two years here at Kansas State University. All of their help and motivation lead to my success in graduate school. I would also like to thank them for all the knowledge they shared with me about not only petroleum geology, but also about life.

I would also like to thank Dr. Deon Van der Merwe for helping me with the FT-IR analysis of my samples and David Hommertzhaim for everything he did to help me collect my samples.

The past two years have been full of school and work, but through all of it I gained friends. These people helped my through coursework, thesis work, and calming my brain work that I could not have tackled without them. For all of this, I have to thank you all.

Lastly, I would like to thank my family and friends for their support throughout my academic career, especially my fiancé, Brien Wilson. If it were not for him, I would never have made it through.

Chapter 1 - Introduction

Paleozoic chert reservoirs with prolific production exist across several provinces of the United States, including the southern mid-continent (Figure 1). There are many fields that produce from the chert in southern Kansas that still provide promise for the future with large amounts of reserves. The Mississippian-aged chert, or chat as it is informally known in the mid-continent, forms an arcuate fairway more than 160 km (Montgomery et al., 1998; Watney et al., 2001) long across the flanks of major late Mississippian – early Pennsylvanian uplifts; these uplifts include the Central Kansas Uplift and the Nemaha Uplift (Figure 2). According to Watney et al. (2001), the name “chat” is used throughout the mid-continent to describe a high-porosity, low resistivity producing chert reservoir. Characteristics of chat reservoirs are unusual, with considerable variability in facies and textures, multiple pore systems, and porosities as high as 30-50% (Montgomery et al., 1998). These Mississippian chat reservoirs are renowned hydrocarbon reservoirs.

The Spivey-Grabs Field (Figure 3) is the largest Mississippi Chat oil and gas field discovered in the mid-continent to date, covering more than 380 km². The field spans southwestern Kingman County and northwestern Harper County with a producing reservoir of clean, porous chat that ranges from 0 to 49 m thick (Frensley and Darmstetter, 1965; Watney et al., 2001). Hydrocarbon production in The Spivey-Grabs field is often complicated by what are observed to be numerous compartments across the field. Because of its past production and future promise, many studies have been completed on the structure, stratigraphy, and geochemistry of biomarkers of the field (e.g. Evans, 2011; Frensley and Darmstetter, 1965;

Harris and Larsh, 1979; Mazzullo e. al., 2009; McIntire, 2014; Montgomery et al., 1998; Rogers et al., 1996; Watney et al., 2001).

Biomarkers, or “biologic markers”, type oil based upon ratios of different carbon chains of oil. Biomarkers are complex molecular fossils derived from biochemicals, particularly lipids, in once-living organisms (Peters et al., 2005) that provide information on the origin, migration history, accumulation and alteration of the crude oil in a reservoir. Biomarkers established by Evans (2011) indicated that Mississippian oil from the Spivey-Grabs field plotted in two distinct maturity groups on a Biomarker Maturation Index graph, a mature group and a less mature group. While studying the biomarkers found in oil can provide oil-to-source rock correlation, analyzing the inorganic constituents of oil, such as rare earth elements (REEs) and trace metal elements (lead, chromium, nickel, K/Rb, Sr/Rb, U/Th ratios, and others) could provide information on the field that has not been looked at before.

It is important to study REE and trace metals in crude oil because of their importance in geochemical characterization of its source and origin (Chaudhuri, 2014; Khuhawar et al., 2012; R. Nakada et al., 2010). REE studies completed on crude oils are becoming more common because of this, but they are still quite limited; major studies are by Abanda and Hannigan (2006), Akinlua et al. (2008), Akinlua et al. (2015), Dao-Hui et al. (2013), Ramirez-Caro (2013), and McIntire (2014). A study of this kind has not been completed on the Spivey-Grabs field.

The primary focus of this research consisted of looking at the inorganic constituents to determine if they could provide a new way to type oils, as well as help explain the observed compartmentalization in the Spivey-Grabs Field. This analysis of the REE and trace metal concentrations of the oils in the Spivey-Grabs Field not only provided a first look at the inorganic constituents of the compartmentalized oils in the field, it was also a first step in

establishing inorganic markers that can provide information and understanding on the source and history of crude oil and prove just as useful as the biomarkers.

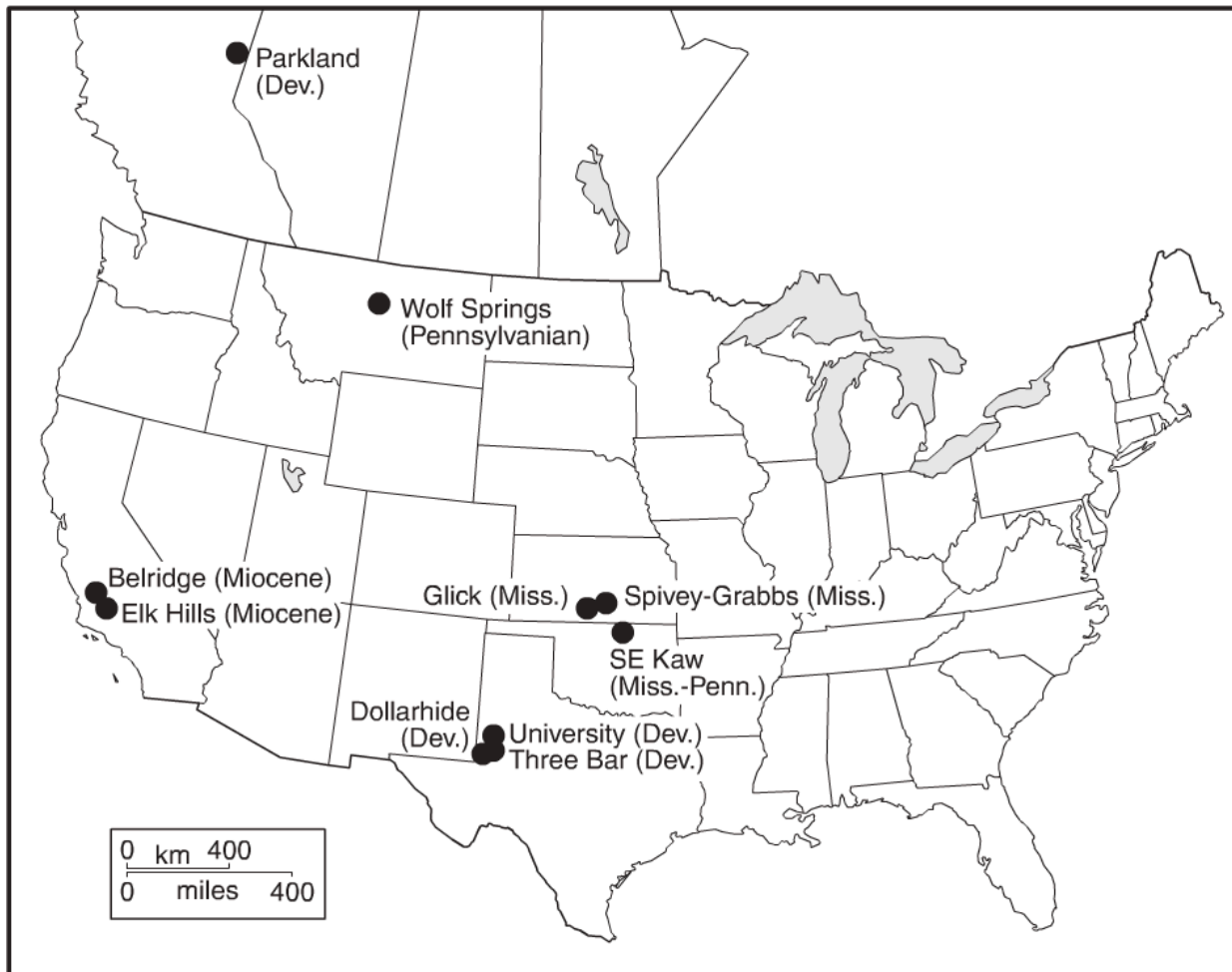


Figure 1. Locations of chert hydrocarbon reservoirs across the United States and Canada (Rogers and Longman, 2001).

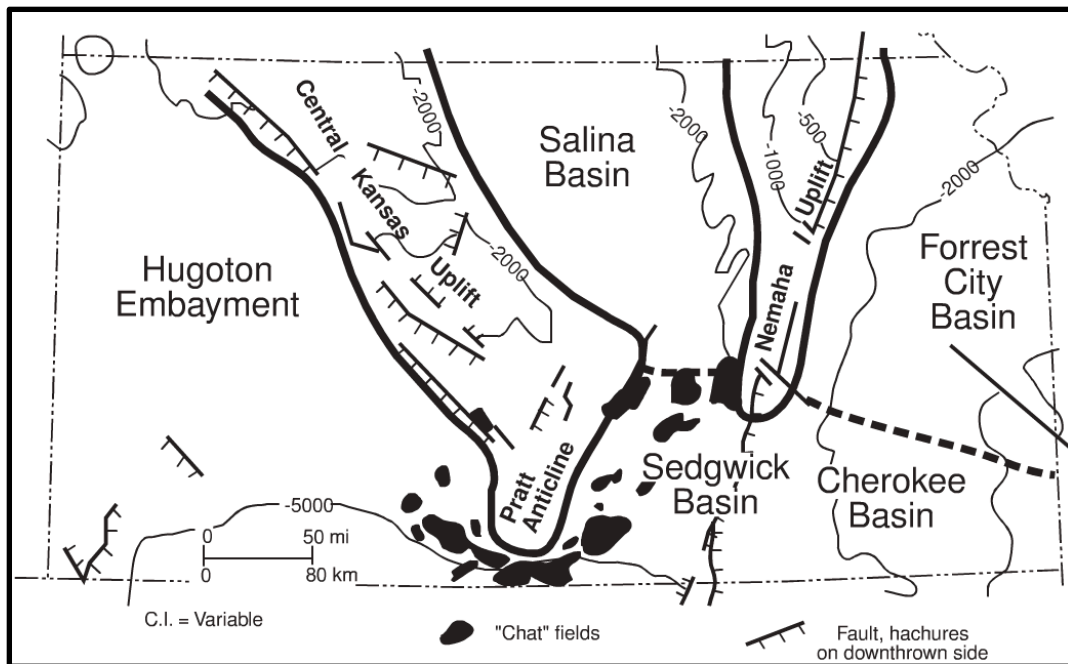


Figure 2. Arcuate fairway of productive Mississippian chat reservoirs shown in relation to regional structures across Kansas (Montgomery et al., 1998).

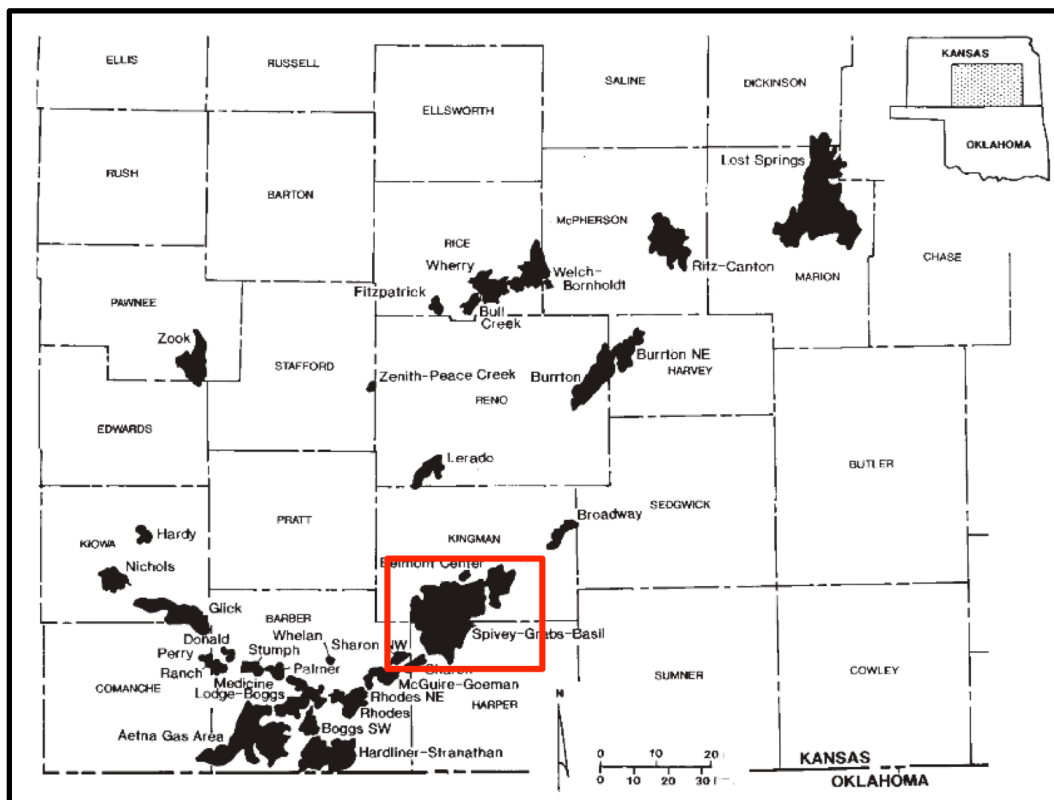


Figure 3. Location of Spivey-Grabs Field in relation to other major chat reservoirs in south-central Kansas. Modified from Montgomery et al. (1998).

Chapter 2 - Background

2.1 Geologic Setting

2.1.1 Regional Environment of Deposition

Very large epicontinental seas covered the continental North American platform throughout Mississippian time (Figure 4). A carbonate shelf covered a majority of the central and southwestern United States with the outer shelf and shelf margin extending into and throughout southern Kansas during Osagean time (Merriam, 1963; Watney et al., 2001; Witzke, 1990). These shallow seas were surrounded only locally by land of high enough elevation to provide clastic detritus, limiting the influx of detrital sediment onto the carbonate shelf. This area of the shelf probably only experienced low- to moderate-energy depositional conditions as a result of the Pratt anticline and Nemaha uplift isolating this embayment (Mazzullo et al., 2009). During the Mississippian, Kansas was located close to the equator (Figure 5) at approximately 20° south latitude (Witzke, 1990); as a result of its location and the lack of clastic deposition, the waters on the shelf were probably moderately warm and predominantly clear (Merriam, 1963; Watney, 2001). According to Watney et al. (2001) and Mazzullo et al. (2009), studies of local areas suggest that this carbonate shelf may have been experiencing transgressive-regressive cycles, which allowed it to be periodically subaerially exposed. These elements provided near perfect conditions for the carbonate deposition.

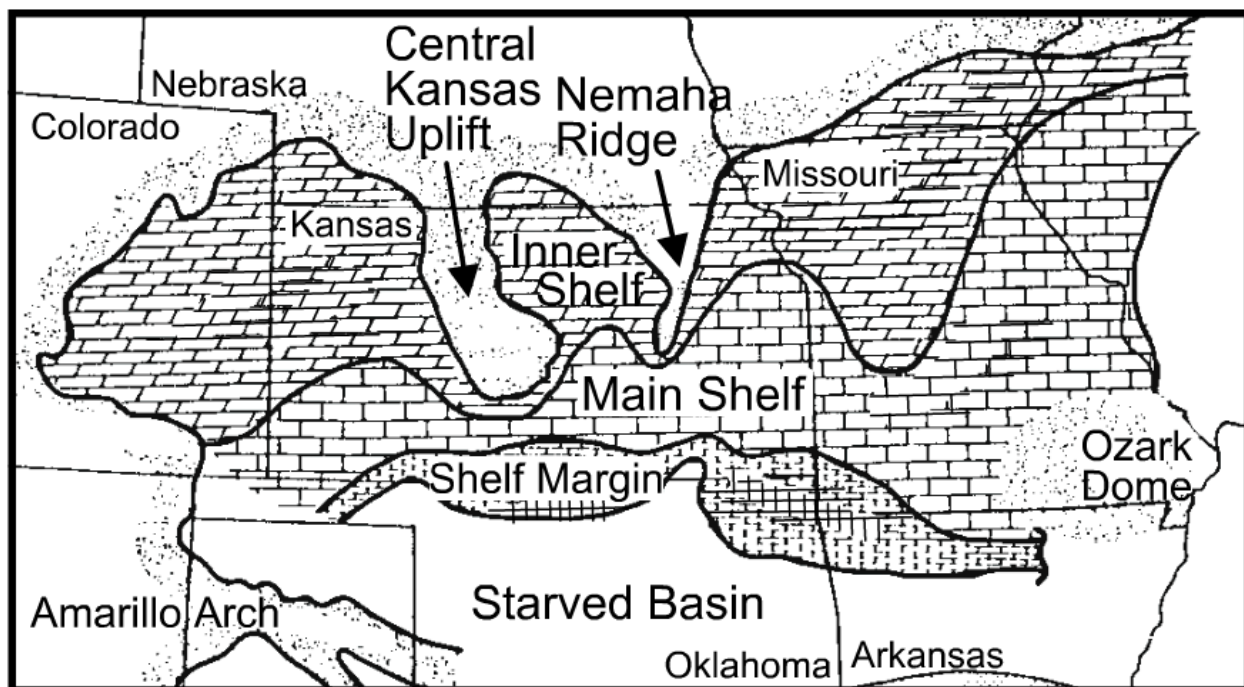


Figure 4. Paleogeographic map showing shelf locations during Mississippian times (Watney et al., 2001).

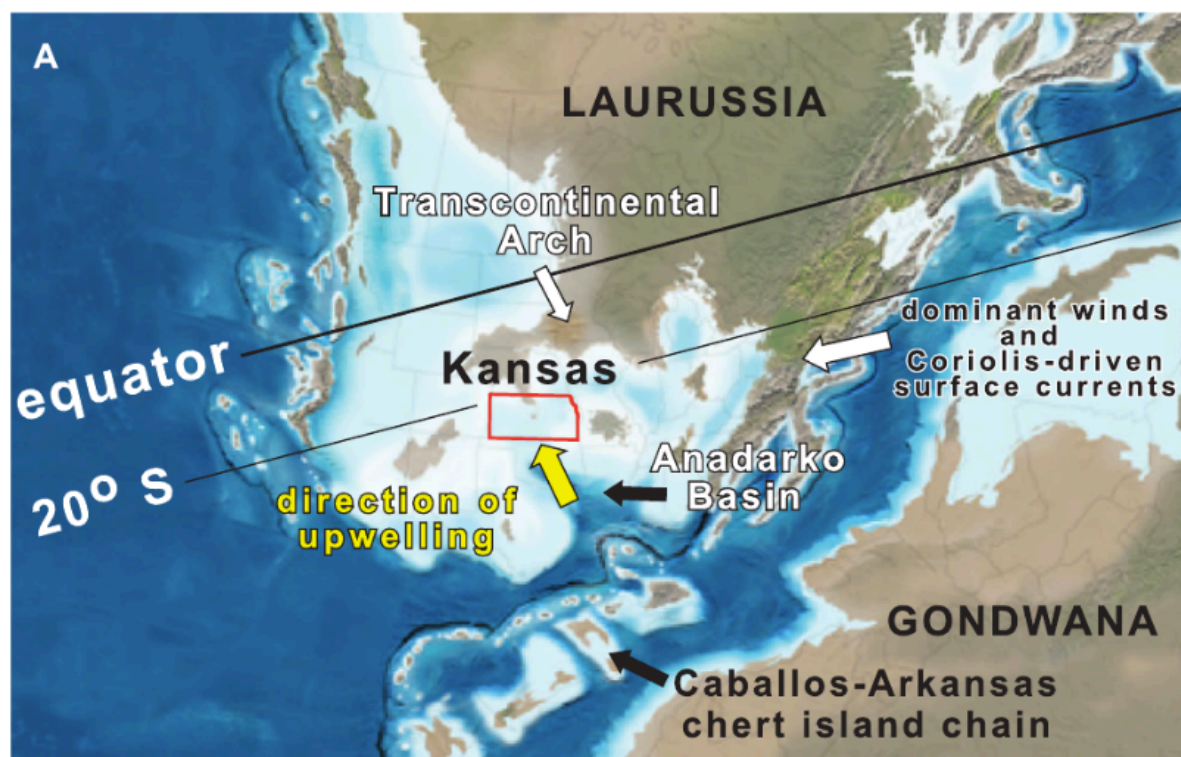


Figure 5. Paleogeographic map showing the location of Kansas and its relation to the equator during Mississippian times (Mazzullo et al., 2009).

A deep seaway lay south of the carbonate shelf along a convergent plate boundary. Volcanic activity occurred along the southern plate of this convergent boundary. Silica resulting from volcanic emissions may have acted as a source of chert in southern Kansas (Scotese, 1999; Witzke, 1990).

Erosion occurred toward the end of Mississippian that persisted through the Early Pennsylvanian. As the seas receded, the Mississippian surface was reduced to a peneplain, a low-relief plain representing the final stages of fluvial erosion during a time of tectonic stability. Fluvial systems eroded sediments from anticlinal peaks, resulting in the bulk of Mississippian deposits remaining in synclinal features (Merriam, 1963).

2.1.2 Regional Stratigraphy

As depicted in Figure 6, Kansas is located on a platform-like extension of a large, stable craton that is a buried southern extension of the Canadian Shield (Harris and Larsh, 1979; Merriam, 1963). This tectonic situation has prevailed since the Pre-Cambrian, and as a result, sedimentary rocks in Kansas primarily consist of thin units that are nearly parallel to each other.



Figure 6. Map of North America showing the location of Kansas in relation to the Canadian Shield and the extension of the shield, the Central Stable Region (Harris and Larsh, 1979).

Mississippian rocks can be found across all of the Kansas subsurface, except for where they have been eroded from the crests of uplifts (Figure 7). The erosional period that occurred at the end of the Mississippian and beginning of the Pennsylvanian removed these rocks from areas of higher elevation, including the tops of the Nemaha Anticline, the Central Kansas Uplift, the Cambridge Arch, and other smaller features (Figure 8). While they are present across the subsurface, Mississippian rocks only outcrop in Kansas in the very southeastern corner of the state in Cherokee County (Merriam, 1963; Watney et al., 2001; Zeller, 1968). According to Zeller (1968) these rocks reach a maximum thickness of more than 1,700 feet in the Hugoton Embayment of southwestern Kansas.

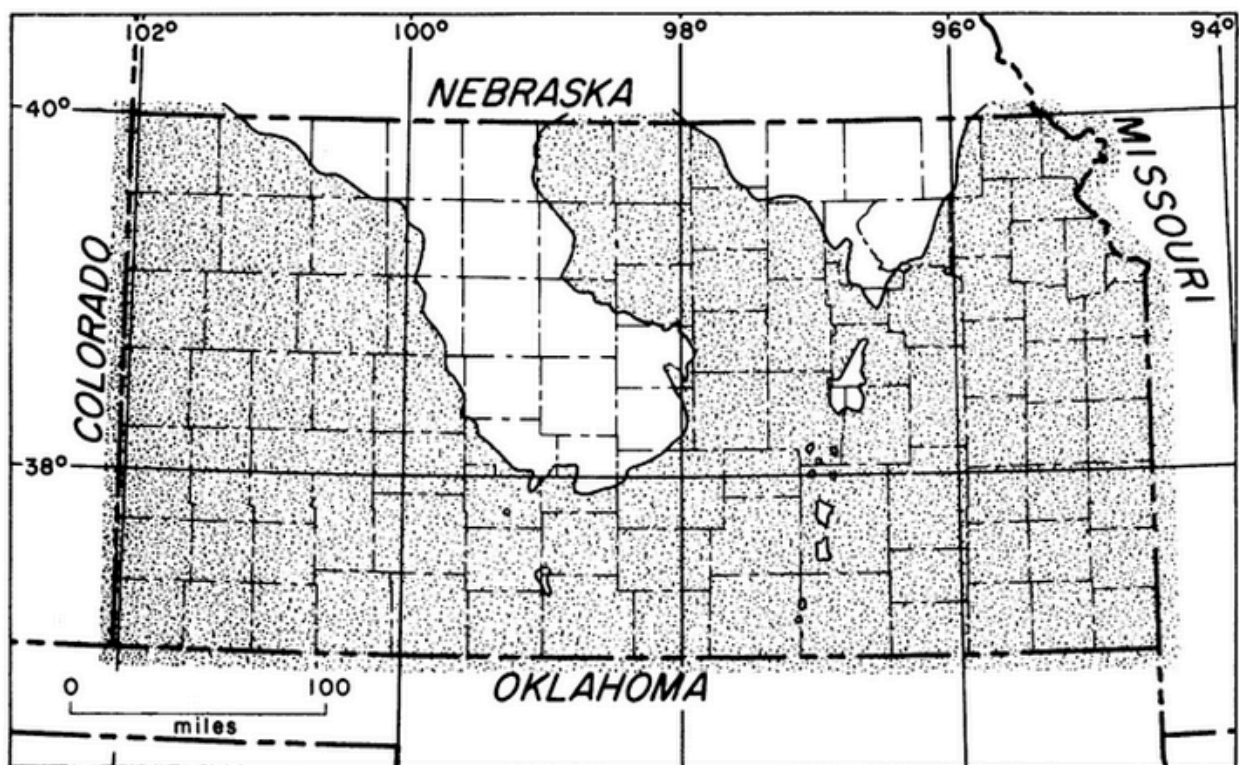


Figure 7. Subsurface extent of Mississippian rocks in Kansas in gray (Merriam, 1963).

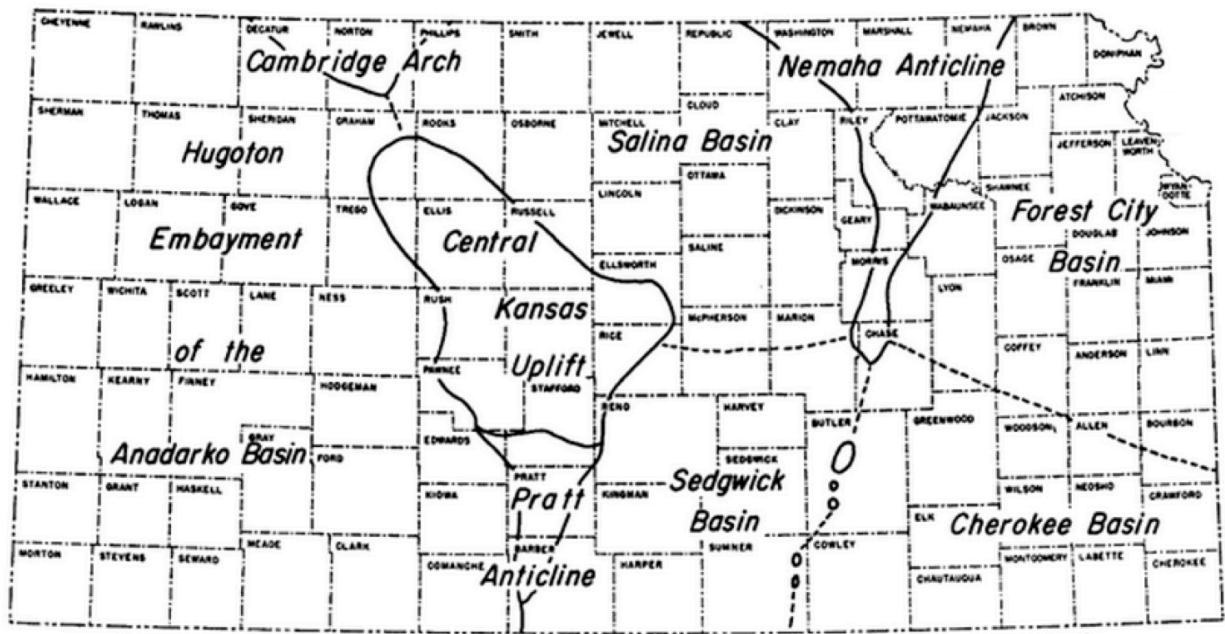


Figure 8. Structural features in Kansas showing uplift features where Mississippian rocks were eroded (Merriam, 1963).

Mississippian deposits in this region are primarily shallow-water carbonates. These rocks would have originated from the deposits of the continental shelf margin that extended through southern Kansas during that time. Older Mississippian rocks are marine in origin, while younger Mississippian rocks are both marine and nonmarine (Merriam, 1963; Zeller, 1968). The older, relatively uniform, widely distributed limestone formations were made from widespread populations of benthonic invertebrates and other marine organisms that secreted hard parts from calcium carbonate and inhabited the shallow carbonate shelf (Merriam, 1963). The mixture of carbonate and clastic sediments from the end of the era probably resulted from the influx of clastic detritus as a result of fluvial erosion that began at the end of the Mississippian.

Mississippian strata in this region lay unconformably beneath Pennsylvanian-aged rocks and above Devonian-aged rocks (Figure 9). The Mississippian system in southern Kansas is composed of four major epochs: the Kinderhookian, the Osagean, the Meramecian, and the

Chesterian (oldest to youngest). The nomenclature for Mississippian units was revised by Maples (1994).

Formations/Members	Age		
Shore Airport Formation	Chesterian	MISSISSIPPIAN	
St. Genevieve Limestone			
St. Louis Limestone \ Stevens Mbr. Hugoton Mbr.	Meramecian		
Salem Limestone			
Warsaw Limestone			
Short Creek Oolite Mbr.	Osagean		
Keokuk Limestone			Cowley Formation
Burlington-Keokuk Limestone			
Burlington Limestone			
Reeds Spring Limestone \ Elsey Fm.			
Pierson Limestone	Kinderhookian		
Gilmore City Limestone			
Sedalia Formation			
Northview Formation			
Compton Limestone	?	?	
Hannibal Shale			
Chattanooga Shale	?	DEVONIAN	

Figure 9. Stratigraphic column depicting Mississippian nomenclature used in Kansas (Evans and Newell, 2013).

The oldest epoch, the Kinderhookian, is comprised of the Hannibal shale, the Compton limestone, the Sedalia dolomite, the Northview formation, and the Gilmore City limestone (oldest to youngest). This Lower Mississippian series consists of beds of shale, limestone, dolomite, and chert in southern Kansas. The Kinderhookian epoch is separated from the overlaying Osagean epoch by an angular unconformity.

While the Kinderhookian-aged formations thicken northward toward a basin in central Iowa, the Osagean-aged formations thicken southward (Goebel, 1971; Zeller, 1968). The Osagean epoch consists of the Pierson limestone, The Reeds Spring limestone, the Elsey formation, the Burlington-Keokuk formation, and the Short Creek Oolite member. The older units in this epoch are only present in the southern portion of Kansas and disappear to the north due to truncation by younger Osagean strata. Osagean-aged formations are composed of dolomite, limestone, chert, and cherty limestone and dolomite beds. The cherty strata are composed of partially dolomitized and argillaceous wackestones and mudstones and partially dolomitized skeletal (primarily crinoidal) packstones and grainstones (Watney et al., 2001; Zeller, 1968) with spiculitic chert present in the uppermost strata (Mazzullo et al., 2009; Watney et al., 2001). The formations in this epoch are often difficult to differentiate from each other; one can often only determine different units based on the characteristics of the included chert (Merriam, 1963; Zeller, 1968). Meramecian-aged rocks disconformably overlie Osagean-aged rocks.

The disconformity between the Osagean and Meramecian epochs is obscured in the northern portion of Kansas and a majority of the period is missing from much of the state (Zeller, 1968). Where they are present, the older units consist of granular, sandy, oolitic, and fossiliferous limestone while the younger units are composed of either interbedded dolomite or

various amounts of chert inclusions within a dolomite and silty dolomitic limestone (Zeller, 1968). The Meramecian epoch consists of three major formations: the Warsaw limestone, the Salem limestone, and the St. Louis limestone (the Stevens and Hugoton Members).

The final stage from Mississippian time is the Chesterian epoch. This epoch is separated from the older rocks below it and the younger rocks above it by unconformities. It consists of only two units, the Ste. Genevieve limestone and the Shore Airport formation. Chesterian units exist as sinkhole fillings (Goebel, 1971) and in the subsurface of Kansas they are only known to exist in deeper parts of the Hugoton embayment (Zeller, 1968). According to Zeller (1968) and Merriam (1963), they are composed of discontinuous beds of sandstone with multi-colored shale beds, as well as interbedded sandy and crinoidal limestones and pale-green shale.

Mississippian strata are often very hard to distinguish from one another, especially in southern Kansas. Because of this, many of them are often grouped into a single formation called the Cowley formation (Mazzullo et al., 2009; Watney et al., 2001). The actual distribution of the Cowley formation across Mississippian strata has also varied over time, but the most recent studies by Mazzullo et al. (2009) suggest that it spans the Upper Osagean and Lower Meramecian times (Figure 10). The Cowley formation is one of the most productive zones of the Mississippian in southern Kansas.

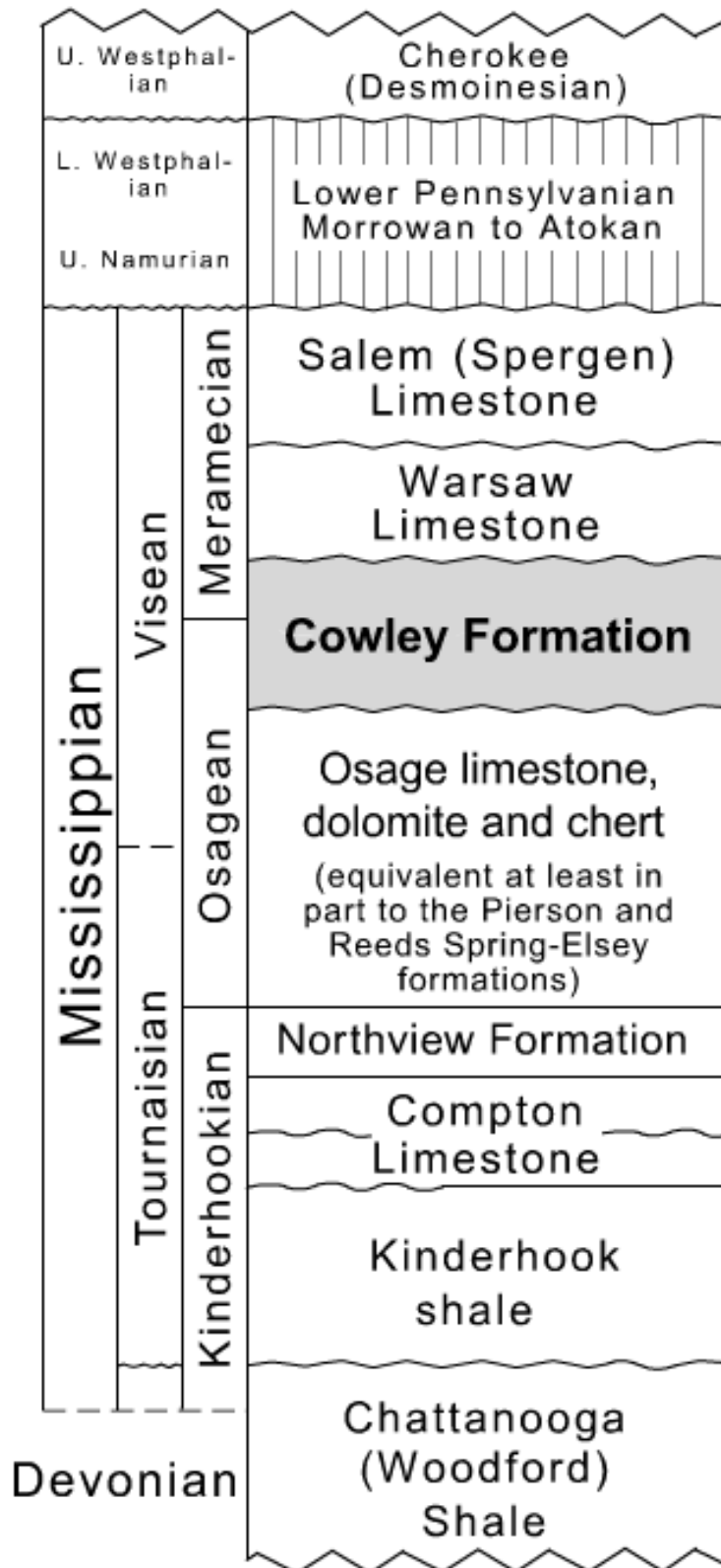


Figure 10. Stratigraphic column depicting Mississippian rocks in Kansas with most recent placement of the Cowley formation shown (Mazzullo et al., 2009).

The Cowley formation contains a thick, approximately 400 ft section of spiculite-dominated rocks. These rocks are derived from demosponges that inhabited the shelf margin in southern Kansas during Mississippian times (Mazzullo et al., 2009). Cowley lithologies are composed of dark to light, slightly calcitic, dolomitic and variably glauconitic and pyritic spiculite, shale, and spiculitic shale that is partially to entirely replaced by chert. The Cowley formation is unconformably bounded and overlies the Osagean limestones and cherts (Lee, 1940; Mazzullo et al., 2009). It onlaps the Osagean, thickening within a paleotopographic low toward the Anadarko basin and thinning out to the northern extent of the formation into central Kansas (Figure 11).

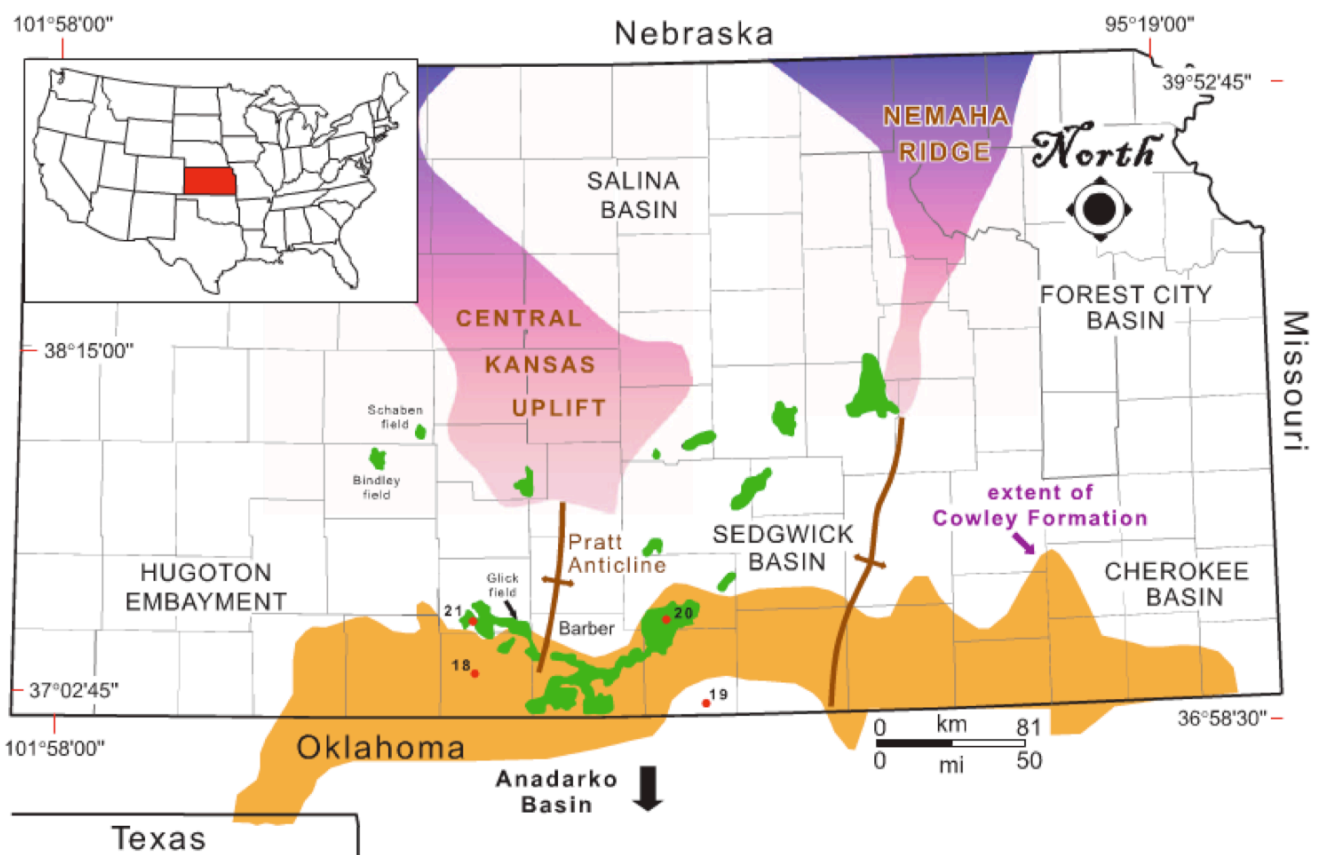


Figure 11. Subsurface extent of the Cowley formation in orange in relation to regional post-Mississippian - pre-Desmoinesian tectonic elements with some of the larger Mississippian chert and/or spiculite oil and gas fields in green (Mazzullo et al., 2009).

According to Mazzullo et al. (2009), the strata in the formation can be divided into four lithologies based on their depositional origins: (1) limestone, (2) bedded spiculite, (3) lenticular- to flaser- to nodular-bedded spiculite and shale, (4) dark gray shale. Most of the spiculite lenses and some associated shale have been partially to completely replaced by chert through three generations of syndepositional and postdepositional silicification. Post-Cowley and pre-Meramecian erosion and the introduction of meteoric waters on the exposed erosional surface allowed alteration of the strata. Diagenesis of the rocks also included several episodes of dissolution and porosity formation, creating the porosity needed to enable the Cowley formation to be a promising reservoir.

2.1.3 The Spivey-Grabs Field

The Spivey-Grabs field is part of a fairway of oil and gas fields producing from the Mississippian chat formations that flank the southern extent of the Central Kansas Uplift (Figures 12). The field is located on the southern flank of the Pratt Anticline and the western flank of the Sedgwick basin and spans approximately 380 km² of southwestern Harper County and northwestern Kingman County. This combination oil and gas field produces from Osagean-aged rocks of the Cowley formation (Harris and Larsh, 1979; Mazzullo et al., 2009; Montgomery et al., 1998). The field exhibits a monoclinical structure with a reservoir thickness that ranges from 0 to 49 m (Frensley and Darmstetter, 1965; Watney et al., 2001). Production across the field is not consistent because it is often disrupted due to the highly “compartmentalized” nature of the field.

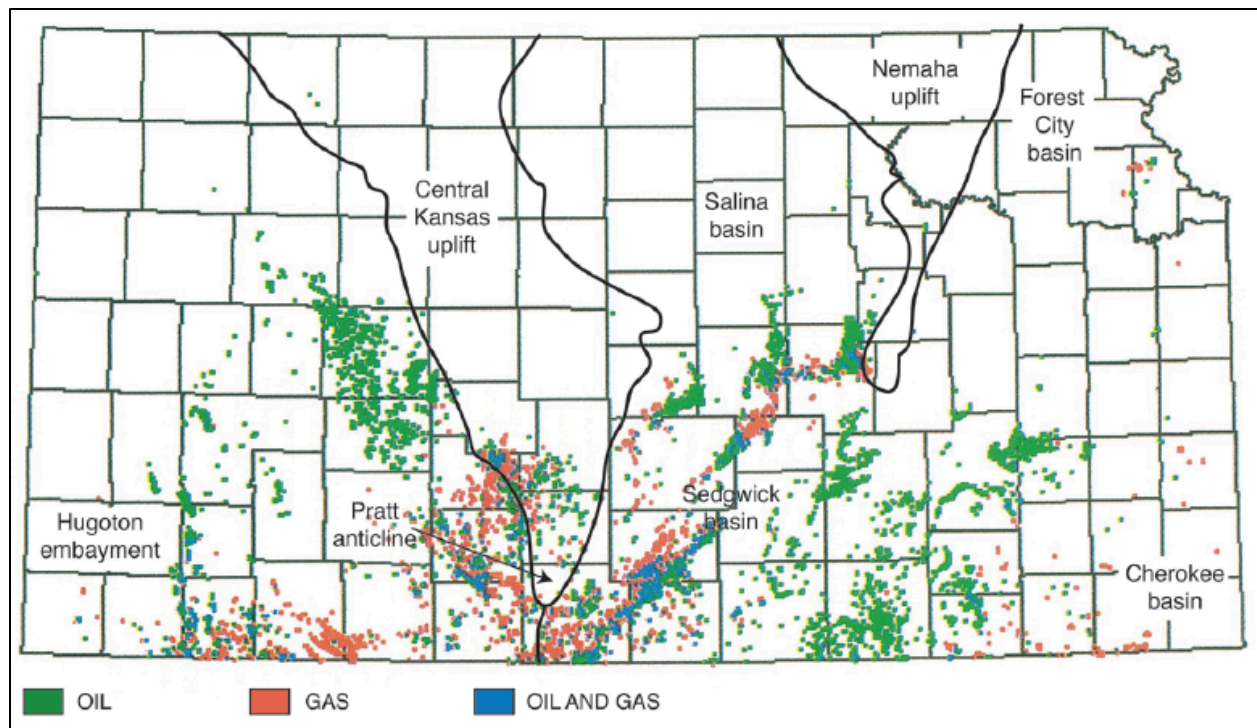


Figure 12. Mississippian oil and gas production locations in relation to major subsurface structural features in Kansas (Evans and Newell, 2013).

The Spivey-Grabs Field has an average porosity of 12% and an average permeability of 37 millidarcies, but porosity levels can reach a high of almost 50% in some areas. Much of the porosity in the chert reservoir exists in the form of micro-pores. Many geologists use the term “tripolitic” chert for this form of highly porous chert (Rogers et al., 1996). The more successful wells within the field have oil production rates as high as 1800 bbl per day. The field also still provides immense promise, with per-well reserves of 50,000 to 1.2 million bbl oil and 0.75 to 20 bcf gas (Montgomery et al., 1998).

Hydrocarbons in the reservoir are contained by stratigraphic traps formed from a series of up-dip porosity pinchouts below an erosional unconformity. The porous area of the field is comprised of chert fragments that are coarsely tripolitic and enclosed in a fine tripolitic chert and tripoli matrix (Frensley and Darmstetter, 1965). The southern limit of the field is defined by an

abrupt change from porous chert to a dense chert, dolomitic mudstone. This change in lithology occurs variably across the field, existing laterally between offsetting wells and isolating areas of higher production rates (Frensley and Darmstetter, 1965; Watney et al., 2001). According to Frensley and Darmstetter (1965), the porous chert reservoir becomes dense or grades into light gray dolomitic chert, cherty dolomite or limestone updip and experiences increasing water saturation downdip, limiting the extent of the field.

The location of oil in the reservoir is complicated by the existence of observed compartments across the field. The location of these compartments seems to strongly affect production, causing variations from well to well. Two wells within a few miles of each other can have completely different production rates. According to Hommertzheimer, the Kingman Production Superintendent of Pickrell Drilling Company, Inc. (personal communication, 2014), one of the wells in the field has high production rates and is nearly free flowing. A second well, so close to the first that you can see it from the well site, is barely producing. There is currently a limited understanding of these compartments, which makes the prospecting and production of oil difficult.

Because the inorganic constituents of the oil in this field have not been previously analyzed, this study provides a first look at the inorganic chemical composition of such an important production resource. Results could provide insight into the origin of the oil and may be able to provide an explanation for the compartmentalization. The Spivey-Grabs field is also a perfect location for this study because an analysis of the organics in the oil has already been completed (Evans, 2011).

2.2 Geochemistry of Crude Oils

Crude oils are composed almost entirely of carbon and hydrogen with sulfur, nitrogen, and oxygen constituting approximately three percent. Metals make up less than 0.1 percent of the constituents of crude oils. Rare earth elements bond with the oxygen and nitrogen in crude oil (Chaudhuri, 2014; Hunt, 1995). The lanthanide elements (Ln) or Rare Earth Elements (REEs) are a group of 14 elements ranging from lanthanum to lutetium (Appendix A). Rare earth elements bond strongly with nitrogen and oxygen, both of which exist in high concentrations in crude oil compared to metals. The REEs that are present in crude oils probably came from organic material before it experienced catagenesis and formed into oil. According to Chaudhuri (2014), REEs reside in the heavy portion of crude oil, allowing for the study and comparison of the relative concentrations of light REEs (LREE), middle REEs (MREE), and heavy REEs (HREE). Trace elements, such as transition metals, also reside in the heavy portion of crude oil. The source rock, type of organic matter, and depositional environment profoundly affect the concentrations and ratios of these elements in crude oils (Lewan, 1984).

Michael McIntire (2014) and Daniel Ramirez-Caro (2013) both analyzed the concentration of REEs and trace metals in crude oil. These were two of the first studies to look at these inorganic constituents as geochemical clues to the differences and history of crude oils in Kansas. In his 2014 study, McIntire found that REEs and other trace metals showed that the Lansing-Kansas City oils are highly diverse. Anomalies of Ce, Eu, Tb, Ho, and Tm varied greatly and the relative distribution patterns of the REEs showed differing patterns in regards to LREEs, MREEs, and HREEs, their patterns ranging from nearly flat to having positive or negative anomalies (Figure 13). His results also displayed a wide range of K/Rb ratios, with a minimum of 877 to a maximum of approximately 2000 (Figure 14). An analysis of the array of REE anomalies, REE relative distribution patterns and K/Rb ratios shows that different zones

within the Lansing-Kansas City formation display distinct REE distribution patterns and K/Rb ratios, indicating that each zone has a distinctly different type of oil.

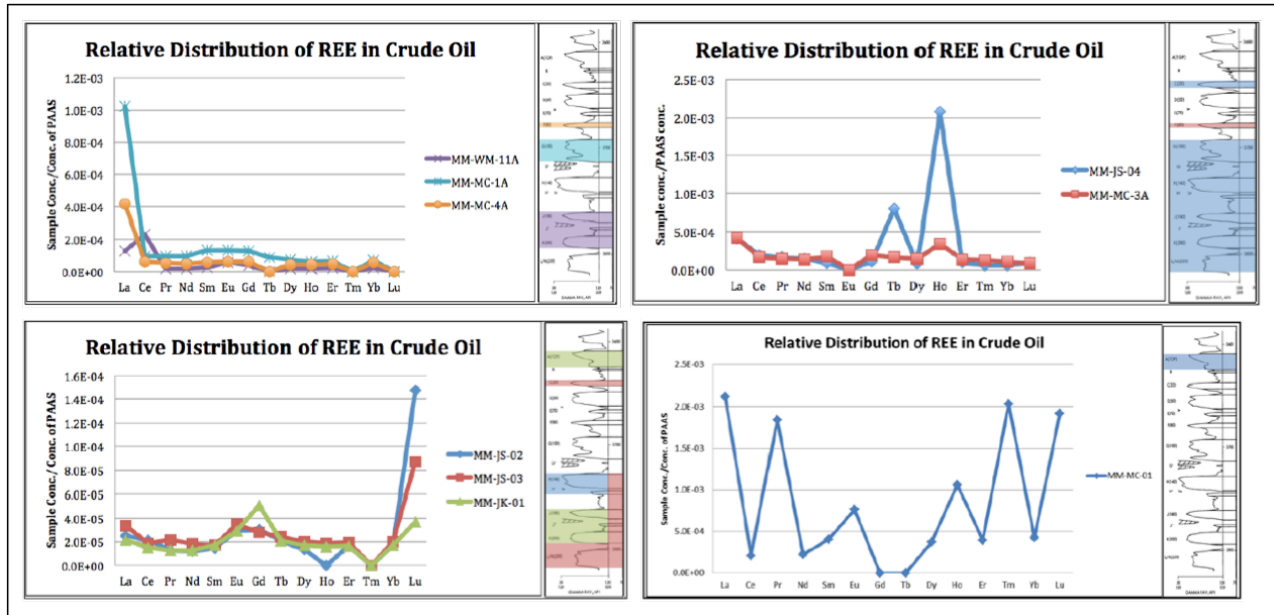


Figure 13. Relative distribution patterns of REEs in crude oil from the Lansing-Kansas City formation. Grouped samples show four distinct zones with similar distribution patterns. Zones of production are highlighted with correlating colors. Modified from McIntire 2014.

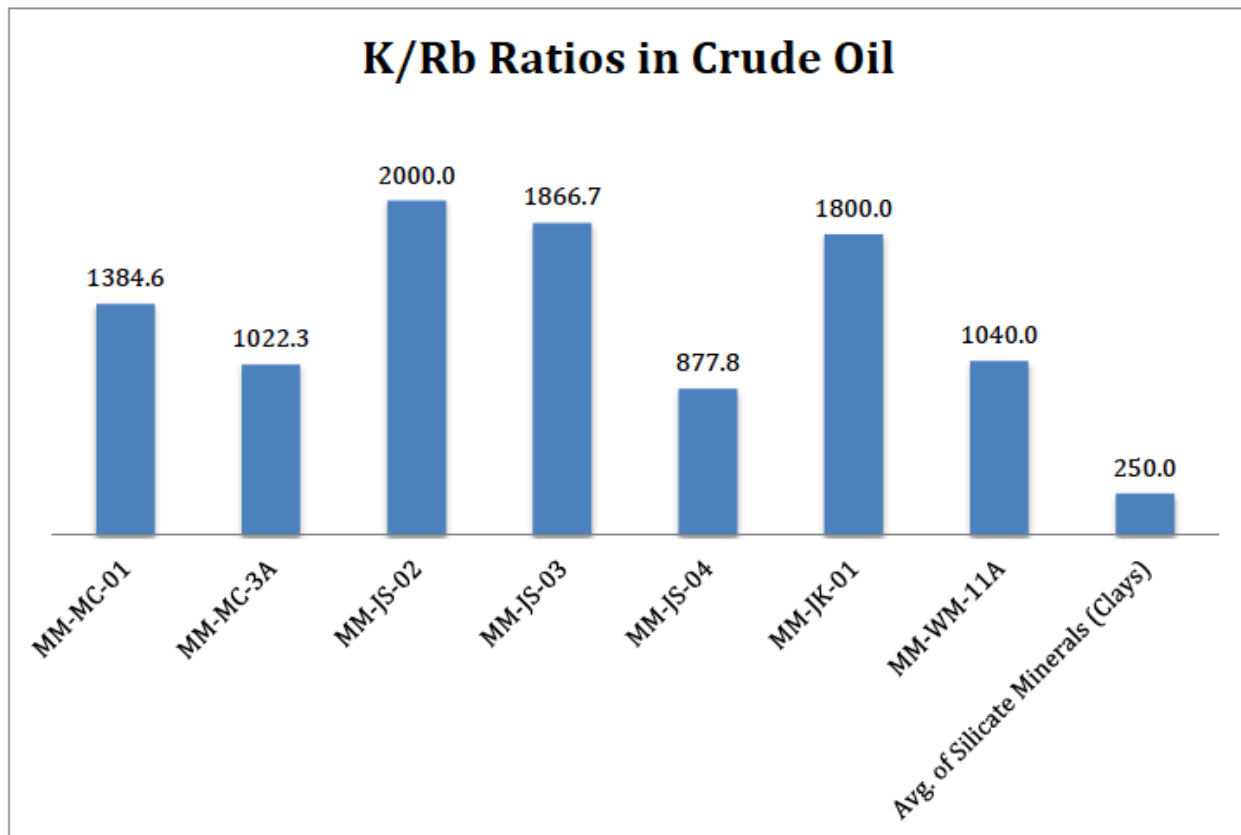


Figure 14. Lansing-Kansas City crude oil K/Rb ratios from McIntire 2014.

Ramirez-Caro (2013) compared Mississippian-aged oil and Devonian Woodford shale oil from the Anadarko basin to determine the relationship between their REE relative distribution patterns (Figure 15). The Mississippian oil samples showed a general LREE enrichment with a minor MREE enrichment and a HREE depletion. A majority of these oils had a negative Ce anomaly and all of the oils showed a positive Eu anomaly. The Devonian oil samples have a LREE enrichment similar to that of the Mississippian, with a more prominent MREE enrichment. Half of the Devonian samples have a depletion in cerium, but, like the Mississippian oils, they all have a Eu enrichment.

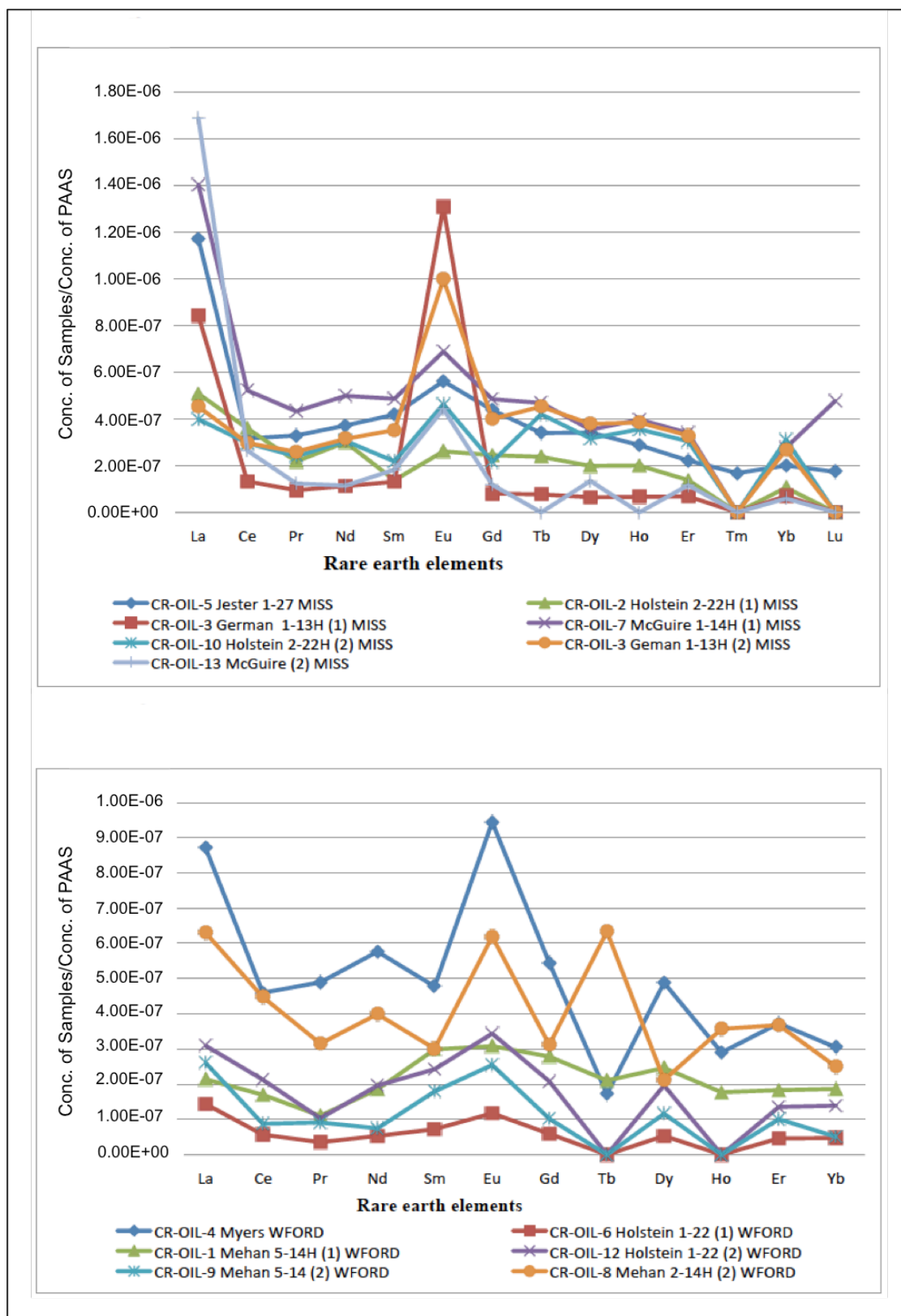


Figure 15. REE relative distribution patterns of Anadarko basin oils from Ramirez-Caro 2013. Top) Mississippian oil samples; Bottom) Devonian Woodford samples.

Chapter 3 - Geochemistry of Spivey-Grabs Oil

Several studies have investigated the depositional, stratigraphic, and structural characteristics of the Spivey-Grabs reservoirs, but the geochemistry of the oils in the field has not been thoroughly studied until recently. A study by Evans (2011) completed a geochemical analysis of oils from this Mississippian play. By studying the results from gas chromatograph mass-spectroscopy (GCMS), Evans completed a biomarker analysis on the organic matter in the oils.

Biomarkers established by Evans (2011) indicated whether the source was immature, early, peak, late, or condensate when catagenesis occurred. His analysis of C₂₉ hopanes, C₃₂ steranes, and trisnorhopanes showed that the samples plotted in two distinct maturity groups (Figure 16); one of the groups plotted as less mature than the other on a Biomarker Maturation Index graph. These results show that areas throughout the field have distinctly different maturation indices. He suggested that two separate oils might have charged the reservoir, and that these oils are probably separated and kept from mixing by the multiple compartments throughout the field.

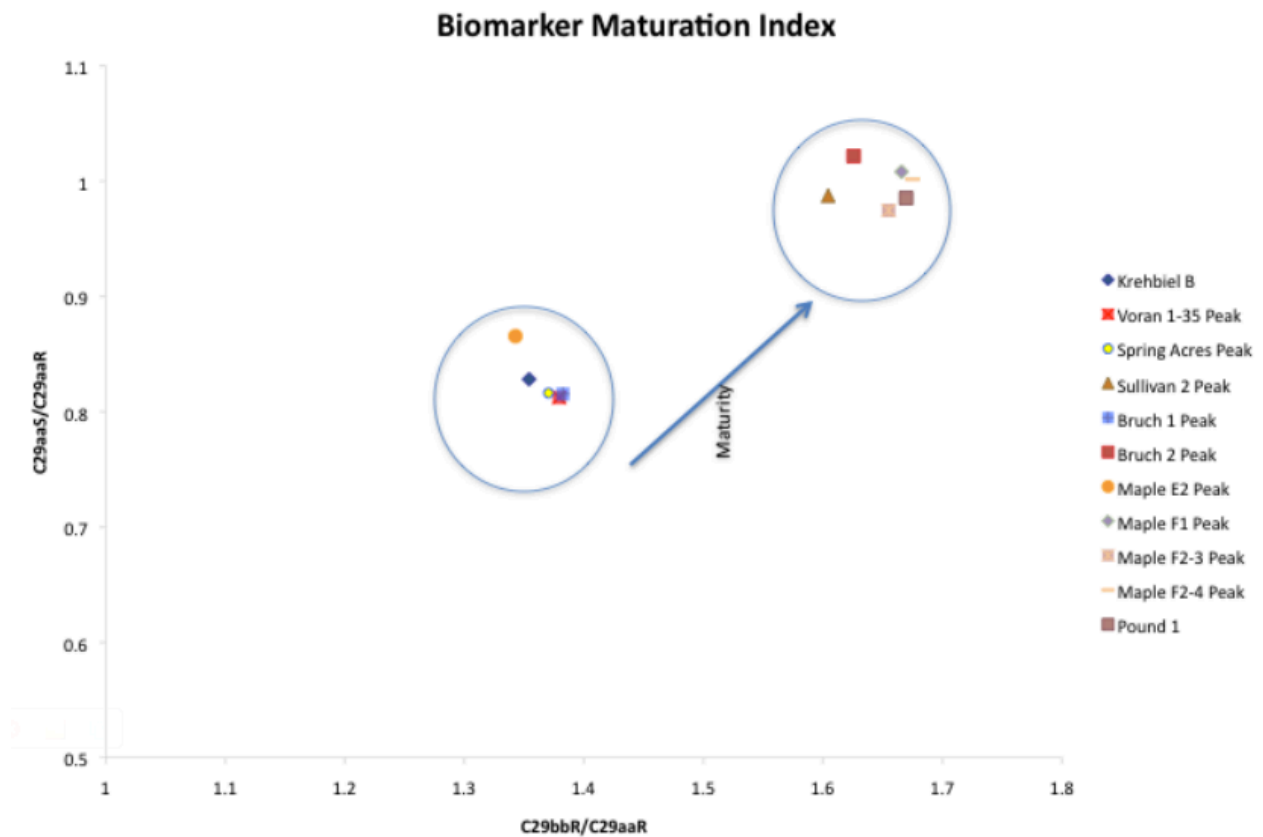


Figure 16. Biomarker Maturity Index with samples displayed from Evans (2011) showing the two maturity indices present in the Spivey-Grabs Field.

Chapter 4 - Methods

4.1 Field Methods

4.1.1 Study Area and Sample Locations

The study area comprised 10 well locations across the Spivey-Grabs Field (Figure 17 and Figure 18). All of the samples were collected in the Kingman County portion of the field. Sample locations were chosen based on the wells sampled and the oils analyzed in Drew Evans' 2011 thesis project. The original goal was to collect oil samples from all of the wells that Evans acquired his samples from. Out of the ten wells Evans sampled and analyzed oil from, three were no longer operated by the same drilling company. Because of this, only seven of the same wells could serve as sample locations for this thesis; three extra sample locations were chosen, for a total of 10 samples (Table 1).

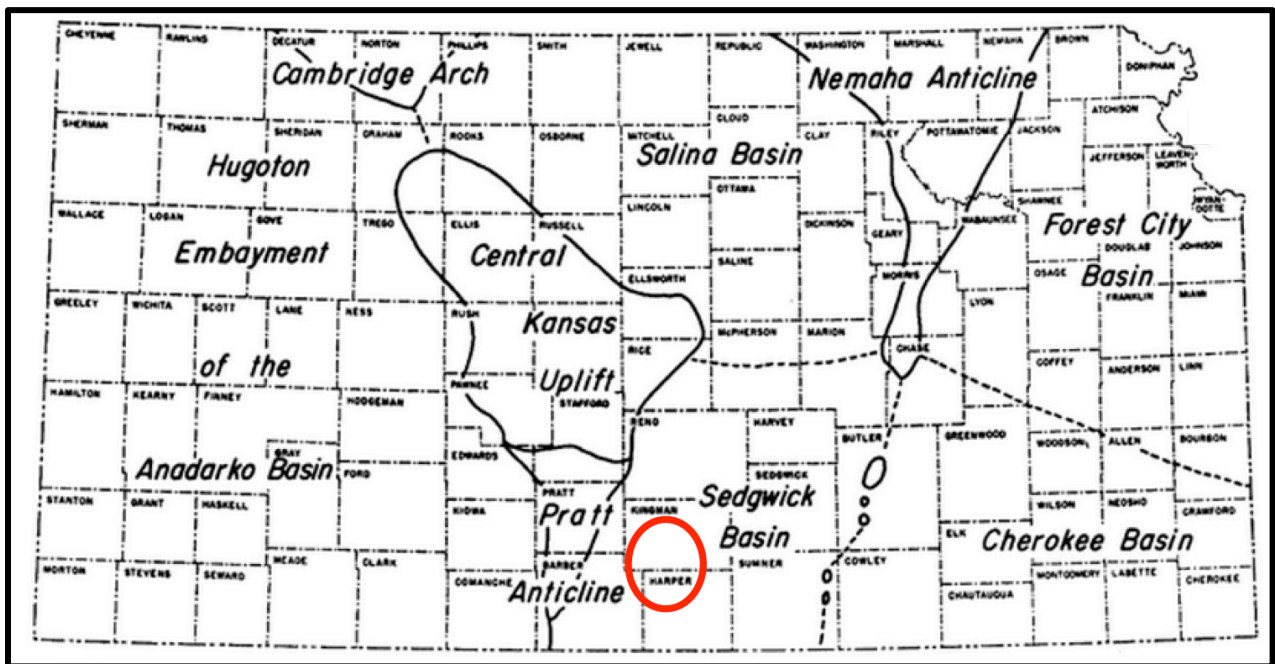


Figure 17. Map of Kansas with sample location in red. Modified from Merriam, 1963.

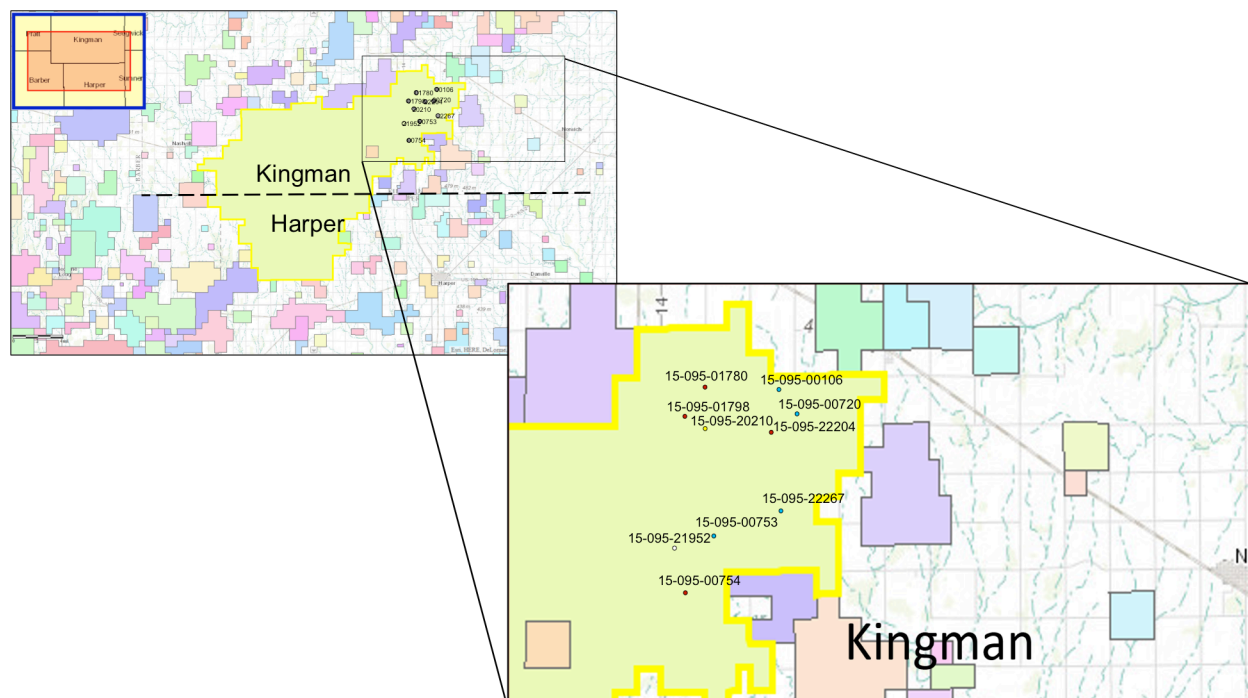


Figure 18. Map showing locations where samples were collected within the Spivey-Grabs Field.

Table 1. Well locations and corresponding samples names. Sample locations also in Evans (2011) are highlighted in blue.

Well Name	API	Latitude	Longitude	Section	TWP	RGE	Sample Name
Bruch No. 1	15-095-01780	37.5070847	-98.0378153	24	29S	7W	BK-14-01
Bruch No. 2	15-095-22119	37.5034500	-98.0398790	24	29S	7W	BK-14-02
Pound No. 1	15-095-00754	37.4702790	-98.0482350	2	30S	7W	BK-14-03
Maple E No. 2	15-095-20210	37.5004200	-98.0434890	25	29S	7W	BK-14-04
Maple G No. 1	15-095-00106	37.4963760	-98.0242890	30	29S	6W	BK-14-05
Maple F No. 1	15-095-00720	37.5006040	-98.0366600	25	29S	7W	BK-14-06
Maple F No. 2	15-095-22204	37.4964280	-98.0371710	25	29S	7W	BK-14-07
Krehbiel B No. 1	15-095-01798	37.4932940	-98.0518870	26	29S	7W	BK-14-08
Coykendall No. 10	15-095-22267	37.4779108	-98.0292353	36	29S	7W	BK-14-09
Krehbiel A No. 1	15-095-00753	37.4711370	-98.052795	2	30S	7W	BK-14-10

4.1.2 Sample Collection

Samples were collected on Saturday, February 15, 2014. Oil was collected directly from the wellhead into 1000 mL Nalgene bottles. In order to collect the oil, the bottle was held two to three inches from the wellhead pipes while the production superintendent from Pickrell Drilling controlled the flow of oil out of the pipe. The quantity of oil that filled the Nalgene bottle was monitored and the oil flow was cut off when the bottle was filled. The bottle was then capped to keep out any dust or grass particles and set aside to allow the gas to escape.

After the gas bubbles had all dissipated and more room was available, the bottles were once again filled with oil until they could not contain anymore. This was repeated until the Nalgene bottles were full. Three to four 1000 mL bottles were collected in this way from each of

the ten wells. Multiple bottles were collected at each well to ensure enough oil was collected to provide 1000 mL of pure oil after the oil was separated from the brine.

4.2 Analytical Methods

4.2.1 Methodology for Infrared Absorption Spectral Analysis

Samples were prepared for infrared absorption spectral analysis by Fourier transform infrared spectroscopy (FT-IR) (Appendix B) by pipetting oil from the 1000 mL Nalgene that it was collected in in the field and transferred into a 50 mL centrifuge tube. One to two centrifuge tubes were prepared for each well. The oil was then centrifuged on high for four hours to ensure it was completely separated from any brine.

The 50 mL centrifuge tubes were taken to the Toxicology section of the College of Veterinary Medicine at Kansas State University. A single drop of oil was extracted with a pipet and placed on the detector, a diamond prism that detects light. From here, the FT-IR spectrometer analyzed the oil for bond variations. The results were examined for any correlation between bond lengths, the organics present in the oil and the results from the inorganic geochemical analysis.

4.2.2 Methodology for REE and Trace Metal Analysis

The oil samples were prepared and processed for geochemical analysis in the chemistry lab in the biochemistry department at Kansas State University. The sample preparation process was the same for each sample and began by setting the sample bottles aside to remain still and unshaken for approximately a month. This was done to allow the oil to separate out from the formation water (or brine) that flowed out of the well with the oil. Preparation continued by extracting the pure oil from the 1000 mL Nalgene bottles used to collect the oil in the field. The oil was extracted from the Nalgene bottles to separate it from the brines. This was accomplished by

carefully pipetting the oil from the top of the bottles and depositing it into 50 mL centrifuge tubes. Instead of extracting all of the oil from each sample bottle, a portion of oil was left so no significant amounts of brine were collected and there was no room for error in the extraction. Oil was transferred into centrifuge tubes until 1250 mL of oil filled a total of 25 centrifuge tubes. Each centrifuge tube had been cleaned and rinsed, first with 6N nitric acid, and then by deionized water.

Each centrifuge tube was then centrifuged on high for at least four hours to ensure no brine remained mixed with the oil. After removing the tubes from the centrifuge, one could see that further separation had occurred; this could be determined because brine was present in the bottom portion of the tubes while oil was present in the top portion. Varying amounts of brine were present in the tubes, with some of them not containing any brine and others containing up to 30 mL of brine. Centrifuge tubes that contained more than 15 mL of brine were not used in order to eliminate any chance of cross-contamination of REEs and trace metals from the brine.

Before transferring pure oil to the Vycor beakers, each beaker was washed thoroughly with Sparkleen and then rinsed with deionized water. The beaker was then placed in a HNO_3 acid bath at 200°C. After an hour, the beaker was carefully removed and rinsed with deionized water. This rid the beaker of any residual particles or dust that could have collected in the beaker. The beakers were then either used right away or covered tightly with Parafilm until oil could be transferred from the centrifuge tubes.

The oil was once again carefully separated from the brine for a final time, ensuring no brine was collected and included in the REE and trace metal analysis. This was completed by pipetting a total of approximately 1000 mL of crude oil from the centrifuge tubes into a 1000 mL Vycor (fused silica) beaker. For tubes that contained brine, pipetting stopped at least 5 mL

above the brine. Even when no brine was found in a tube, pipetting stopped at the 5 mL mark. This ensured that no brine had been collected and that the crude oil was completely separated.

After the beakers were filled with oil, the separation process was completed and the evaporation process began. The beaker was placed on a hot plate under a fume hood and heated to a temperature of 100°C. The sample was left at this temperature for 24 hours. Beginning the evaporation process at lower temperatures kept the oil from heating up too fast and boiling or catching on fire; if this occurred, the heavy fraction of the oil would burn, causing the sample to be compromised and no longer acceptable for analysis. The temperature was increased in 30°C to 40°C increments each time the sample stopped smoking until a maximum temperature of 550°C was reached. Once this temperature was reached, the sample remained on the hot plate until it no longer fumed. The smoking occurred as a result of the lighter fractions of the oil being volatilized, leaving just the heavy fraction of the oil in the beakers (Figure 19). This evaporation process took between three and six weeks per sample.

After the light fraction was evaporated and only the heavy fraction remained in the beaker, the sample no longer appeared as a liquid; it became highly viscous, often evaporating until becoming hardened. At this point, HCl and concentrated double vacuum distilled Veritas HNO₃ were combined in a 3:1 (respectively) mixture to form Aqua Regia. The samples were then saturated with 15 mL of Aqua Regia and approximately 50 mL of deionized water. The volume of water added to the sample depended on how much was needed to saturate the sample, and ranged between 15 and 60 mL. The sample was then mixed so the Aqua Regia separated the REEs and trace elements from the solids. The liquids were then collected and the solution was filtered through 42 mm hardened ashless filter paper to ensure any solids that came out with the

liquids were removed. After the sample was completely filtered, the filter paper was rinsed with 1 mL Aqua Regia to release any metals remaining on the paper into the collected portion.

Once this was completed, the sample solution was collected and transferred to a 100 mL Vycor crucible that had also been cleaned in a HNO_3 acid bath. The solution was then evaporated on a hot plate until it was completely dry. After the solution dried and the crucible cooled to room temperature, 10 mL of Aqua Regia was added to each crucible and swirled around to ensure that the evaporated solution dissolved completely. Finally, this 10 mL final solution was collected in a 30 mL Nalgene bottle and sent to the University of Strasbourg for analysis by inductively coupled plasma mass spectrometry (ICP-MS) and inductively coupled mass spectrometry atomic emission spectroscopy (ICP-AES). These instruments show an analytical error of 5%. All samples were prepared and processed in this same way.

Some of the samples separated out into two distinct types of oil after being allowed to sit for a few weeks. These samples appeared to consist of a light oil and a heavy oil. Some of these samples were separated before analyzing, with the heavy portion and light portion being studied individually. If the oil was too thick to be pipetted, it was transferred by pouring it from the Nalgene bottle into the centrifuge tube. For samples that were separated, the light portion of the oil was denoted as sample A and the heavy portion of the oil was denoted as sample B for that sample number. These samples included BK-14-03, BK-14-06, and BK-14-09. However, technical difficulties were experienced while preparing BK-14-09B and, therefore, the sample was not sent for analysis.

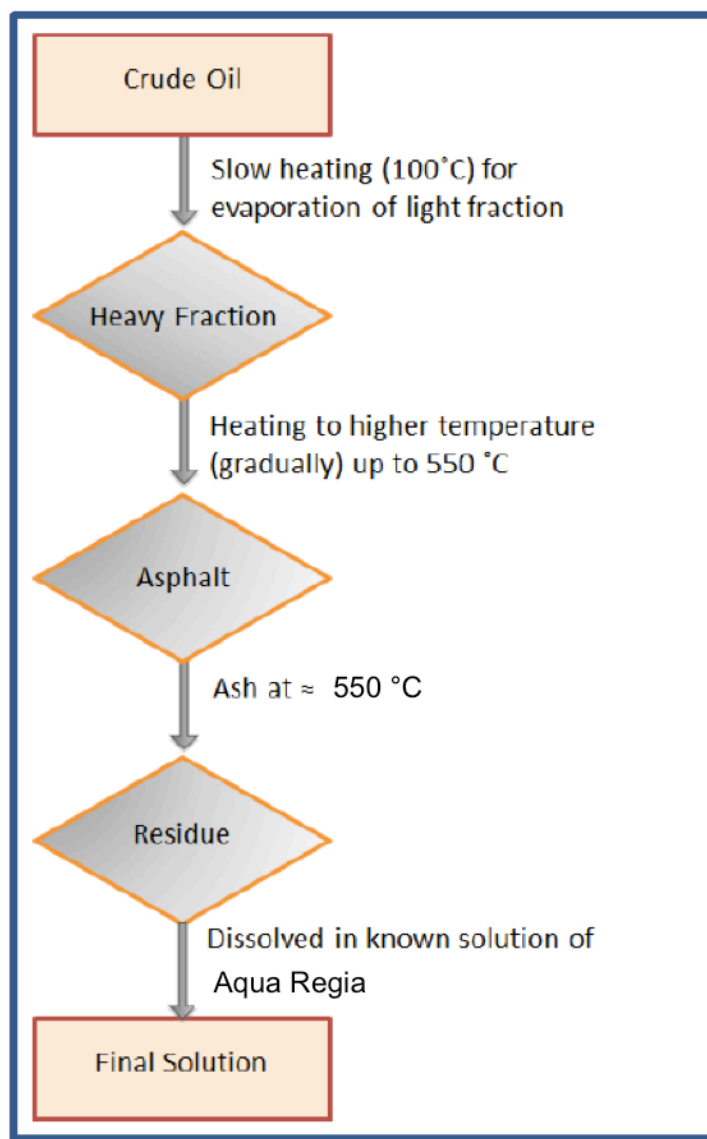


Figure 19. Oil separation flowchart showing strategies of methods. Modified from Ramirez-Caro (2013).

4.2.3 Potential Sources for Analytical Error

There are a number of potential sources for analytical error. The first source of potential error in REE concentration is contamination from the solvent (nitric acid) used to dissolve the ashed crude oil. The nitric acid used in this study is vacuum-sealed, double distilled, VERITAS purified, concentrated nitric acid. A blank sample of this nitric acid was analyzed on the ICP-

MS and the total REE concentrations were only 2.5 ppb. This small amount of REEs would have little affect on the REE patterns of the oil samples. Furthermore, the amount of acid used with the 1000 mL of oil for each sample in this study is the same amount that was run on 200 mL of oil used in previous studies. Any REE concentrations (whether from the nitric acid, hydrochloric acid or the oil) were too low to detect with 200 mL of ashed oil. If the nitric acid did not affect REE within 200 mL of oil, it would most likely not affect 1000 mL of crude oil.

The second concern arises from possible contamination by variable silicate dust. To ensure no contamination occurred from soiled lab materials, before each step of sample preparation every instrument was thoroughly washed, given an acid bath, and then rinsed with deionized water. Great care was taken throughout the preparation of the samples to avoid any possible dust contamination. Any small amount of dust that did happen to get into the samples would have little to no affect on the results because it was accounted for by the Post Achaean Australian Shale (PAAS) standard that was used in the study to normalize the REE distribution patterns found in the oils and correct for any unusual results.

Chapter 5 - Results

5.1 Physical Characteristics of Crude Oils

After the oil was collected from the wellhead, it was brought back to the biochemistry department at Kansas State University. It was then left to sit for a few weeks so the oil and brine could separate as much as possible before being centrifuged. Many of the samples ended up not only separating out into oil and brine; these samples were composed of two distinct oils (Figure 20). These sample bottles contained brine, a light oil (low viscosity), and a heavy oil (high viscosity). The type of oil that was collected at each well is indicated in Table 2. The apparently heavy oil in some samples was so thick that it could not be removed by pipet and reached the viscosity and consistency of peanut butter.

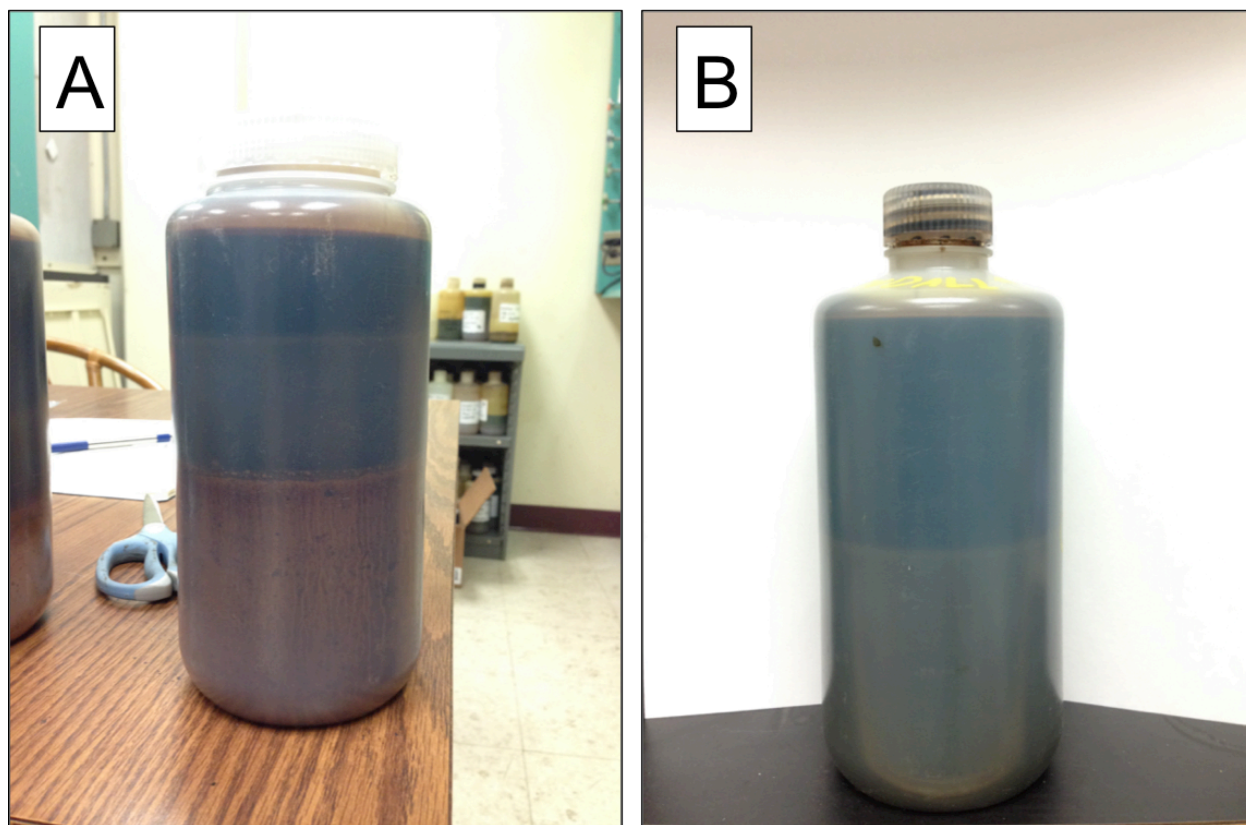


Figure 20. Oil Samples with both heavy and light oil. A) is sample number BK-14-03 and B) is sample number BK-14-09.

Table 2. Physical Characteristics of Oils from Spivey-Grabs field.
Samples also in Evans (2011) are highlighted in blue.

	Well Name	Oil Type
Sample Number		
BK-14-01	Bruch No. 1	Light
BK-14-02	Bruck No. 2	Light
BK-14-03	Pound No. 1	Both
BK-14-04	Maple E2	Both
BK-14-05	Maple G1	Light
BK-14-06	Maple F1	Both
BK-14-07	Maple F2	Light
BK-14-08	Krehbiel B1	Both
BK-14-09	Coykendall 10	Both
BK-14-10	Krehbiel A1	Heavy

5.2 Infrared Spectroscopy Results

A Fourier-transform infrared spectroscopy study of crude oils from the Spivey-Grabs field provides insight into the functional groups (Appendix C) of organic compounds within the oils (Figure 21). A set of three peaks is present between 3000 cm^{-1} and 2700 cm^{-1} for all fourteen of the samples. Five out of the fourteen samples have a peak at approximately 3400 cm^{-1} and a peak at approximately 1635 cm^{-1} that the other nine samples do not display.

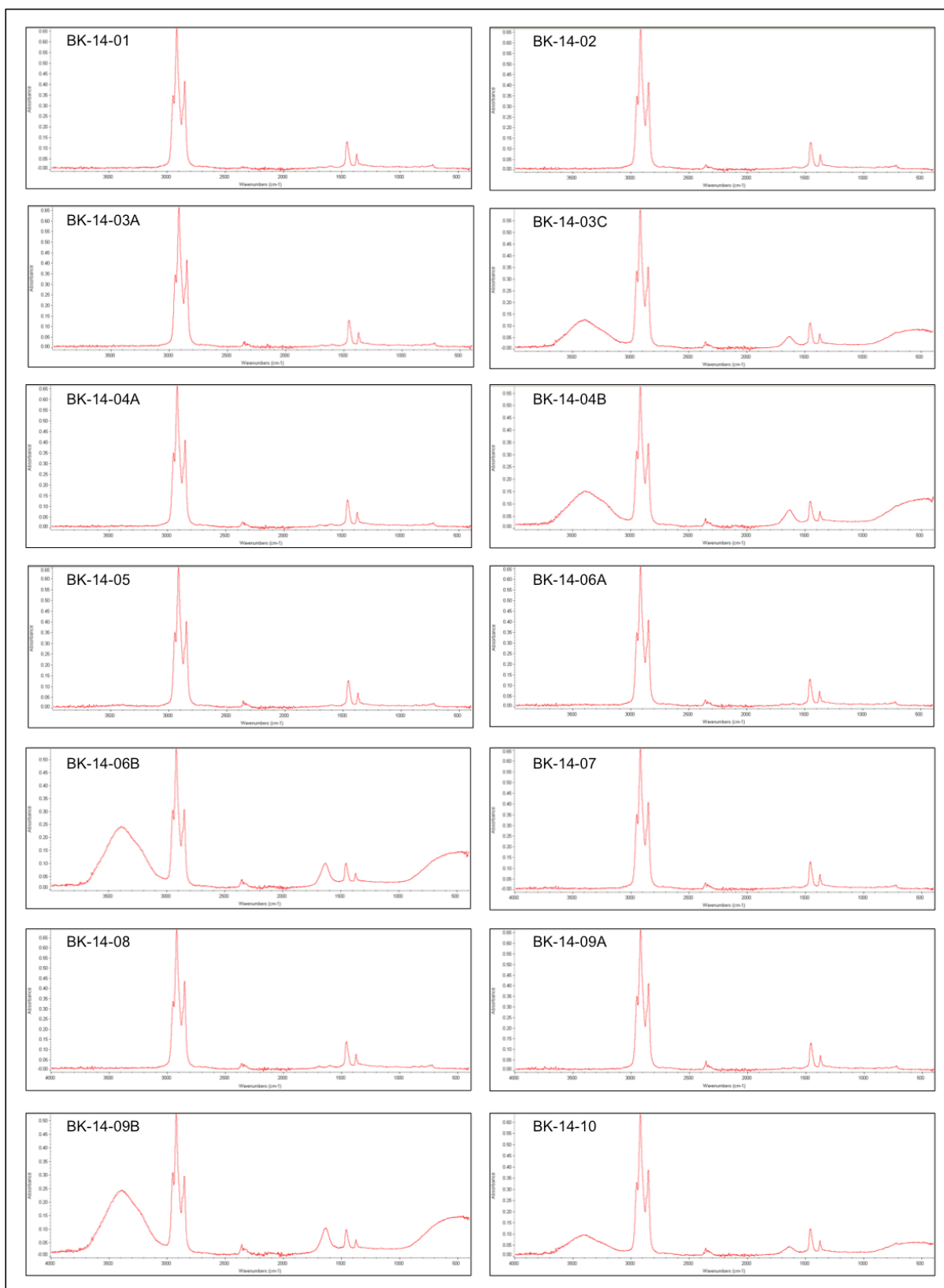


Figure 21. FT-IR spectra for each of the samples analyzed.

5.3 REE and Trace Metal Concentrations in Crude Oils

Raw data was received from the University of Strasbourg after the samples were analyzed by ICP-MS and ICP-AES. REEs were analyzed by ICP-MS because REE contents in crude oils are very low (ppb or even ppt) and ICP-MS is more sensitive than other techniques, allowing it to analyze most of the elements (Soin et al., 2012; Khuhawar et al., 2012). This data was then adjusted to represent the original volumes of each sample. Table 3 displays the adjusted data from the ICP-MS results and Table 4 displays the adjusted data from the ICP-AES results. Only 12 REE were identified: La, Ce, Pr, Nd, Sm, Gd, Tb, Dy, Ho, Er, Yb, and Lu. Those that were not determined had concentrations that were below the detection limits of the instrument. Trace metal element concentrations in Bk-14-02 were all too low to detect. ICP-MS results were not received for BK-14-04, BK-14-03B, BK-14-06B, and BK-14-10 due to technical difficulties. The orange cells in both tables represent elemental concentrations that were below instrumentation detection limits.

Table 3. REE and trace element analytical results for oil from the Spivey-Grabs Field. Concentrations in ppb. REEs are highlighted by red box. Samples also in Evans (2011) are highlighted in blue.

		BK-14-01	BK-14-03A	BK-14-05	BK-14-06A	BK-14-07	BK-14-08	BK-14-09A
Element	Isotope							
Rb	85	1.10E-02	6.25E+00	7.85E-03	7.46E-02	6.80E-03	1.09E+00	1.45E-02
Y	89	3.55E-04	3.09E-02	2.45E-04	5.56E-04	8.26E-03	2.03E-02	7.10E-04
Zr	90	1.15E-02	8.00E-03	-	-	-	2.11E-02	-
Cd	111	1.11E-01	1.00E-02	3.70E-03	2.05E-03	3.70E-03	4.89E-03	1.80E-03
Sn	118	2.58E-02	1.16E-01	7.35E-03	2.10E-02	1.32E-01	7.33E-01	1.76E-02
Sb	121	2.30E-02	4.24E-02	1.68E-02	2.40E-02	3.37E-02	7.38E-02	8.90E-03
Cs	133	1.45E-03	5.90E-01	9.25E-04	9.66E-03	8.50E-04	1.26E-01	1.35E-03
La	139	1.15E-03	7.45E-03	7.25E-04	7.80E-04	3.07E-02	9.72E-03	8.00E-04
Ce	140	2.11E-02	6.22E-02	1.88E-02	3.84E-02	7.95E-02	6.54E-02	3.43E-02
Pr	141	1.20E-04	9.20E-04	4.50E-05	9.76E-05	6.49E-03	1.64E-03	1.20E-04
Nd	146	5.00E-04	3.00E-03	2.65E-04	4.98E-04	1.75E-02	7.38E-03	5.90E-04
Sm	147	7.00E-05	8.20E-04	5.50E-05	1.37E-04	7.00E-05	1.49E-03	3.60E-04
Eu	153	-	-	-	-	-	-	-
Gd	157	7.50E-05	6.30E-04	7.50E-05	7.80E-05	2.30E-03	1.58E-03	1.60E-04
Tb	159	-	1.10E-04	-	-	6.00E-05	4.11E-04	-
Dy	163	5.00E-05	4.00E-04	-	-	1.50E-04	1.23E-03	1.00E-04
Ho	165	2.00E-05	5.00E-05	-	-	-	7.44E-04	-
Er	166	3.50E-05	2.10E-04	2.50E-05	-	1.40E-04	5.78E-04	4.00E-05
Tm	169	-	-	-	-	-	-	-
Yb	172	3.50E-05	3.20E-04	-	-	-	3.78E-04	-
Lu	175	1.50E-05	6.00E-05	-	-	-	-	-
Pb	208	2.36E-01	1.02E+01	1.32E-01	4.54E-01	1.41E+00	7.50E+00	1.01E-01
Th	232	-	-	-	-	-	-	-
U	238	2.10E-02	4.94E-02	1.96E-02	4.14E-02	3.99E-02	5.56E-02	3.28E-02
Total REE		2.31E-02	7.61E-02	2.00E-02	4.00E-02	1.37E-01	9.02E-02	3.64E-02
K/Rb		18182	2864	24204	10850	44118	3888	24138

- below detection limit

Table 4. Trace element analytical results for oil from the Spivey-Grabs Field. Concentrations of Si to P in ppm. Concentrations of Sr to Cu in ppb. Samples also in Evans (2011) are highlighted in blue.

	BK-14-01	BK-14-03A	BK-14-05	BK-14-06A	BK-14-07	BK-14-08	BK-14-09A	BK-14-03C	BK-14-04	BK-14-06B	BK-14-10
Element											
Si	0.0008	0.0130	0.0005	0.0034	0.0045	0.0306	0.0040	0.0595	-	0.2720	0.0111
Al	0.0025	0.0046	0.0025	0.0022	0.0033	0.0096	0.0041	0.0055	0.0135	0.0291	0.0027
Mg	0.0625	7.8000	0.0269	0.0346	0.0183	2.6333	0.0187	147.1429	10.4211	152.5333	12.8511
Ca	0.4625	345.0000	0.4990	2.8224	0.6330	104.4444	0.7280	1138.0952	58.8421	738.6667	295.5556
Fe	0.0255	1.3180	0.0300	0.1746	0.0730	2.3156	0.0730	1.0060	1.2147	5.8133	0.0680
Mn	0.0006	0.1250	0.0005	0.0015	0.0007	0.0281	0.0010	0.0494	0.0136	0.1413	0.0057
Ti	-	-	-	-	-	-	-	-	-	-	-
Na	25.5000	s	11.6000	116.0976	3.3450	s	9.1800	459.5238	425.2632	696.0000	786.6667
K	0.2000	17.9000	0.1900	0.8098	0.3000	4.2556	0.3500	35.4762	1.8947	24.8000	9.3333
P	0.0200	0.0495	0.0038	0.0059	0.0290	0.0256	0.0035	0.0043	0.5065	0.1315	0.0493
Sr	38.0000	s	29.5000	151.2195	22.5000	s	36.9000	36190.4762	3431.5789	32800.0000	9066.6667
Ba	0.8000	38.1000	0.6000	1.2683	0.9000	12.2222	0.7000	72.2143	13.7263	146.0000	19.0889
V	12.6500	34.3000	22.1500	24.3902	7250.0000	7277.7778	38.8000	364.7619	9431.5789	3413.3333	3.3333
Ni	4.4000	65.3000	2.1500	1.7561	1870.0000	1733.3333	8.3000	94.7619	2357.8947	743.2000	0.8889
Co	0.4000	2.3000	0.2500	0.4878	11.3000	10.5556	0.5000	0.2381	13.4737	4.2667	-
Cr	0.5000	243.0000	1.0000	0.9756	1.0000	2.5556	14.3000	0.9524	1.0526	4.5333	1.3333
Zn	23.6500	39.0000	5.9000	23.4146	176.5000	126.6667	14.3000	185.2381	114.3158	182.6667	3.1111
Cu	8.0000	126.0000	8.5000	72.1951	978.0000	390.0000	73.0000	315.4762	1836.0000	676.8000	38.4444

-	below detection limit
s	saturated

Chapter 6 - Discussion

6.1 Two Types of Oil in the Spivey-Grabs Field

6.1.1 Physical Characteristics of Oil

The oil collected from the Spivey-Grabs field displayed varying physical characteristics. Oil samples were collected directly from the wellhead and appeared to be the same, but after being exposed to surface temperatures and pressures for approximately 30 days, clearly separated out. Four of the samples, BK-14-01, BK-14-02, BK-14-05, and BK-14-07, only contained light (low viscosity) oils. Five of the samples, BK-14-03, BK-14-04, BK-14-06, BK-14-08, and BK-14-09, all had a mix of light and heavy (high viscosity) oil. The tenth sample, BK-14-10, only contained heavy oil. The two distinctly different viscosities of oil in the field suggest the two oil groups have different degrees of maturation because the extent of thermal maturation affects API gravity, therefore affecting viscosity (Peters et al., 2005; Peters et al., 2012). The different API gravities of the oils could point to one of three things: 1) the oil in the Spivey-Grabs field underwent alteration within the reservoir after migration; 2) the oil in the Spivey-Grabs field originated from multiple sources; 3) the oil in the Spivey-Grabs field originated from two different pulsing events of the same source.

The varying degrees of API gravity found among the oil samples could provide an explanation for the compartmentalization of the Spivey-Grabs field. The heavier oil could be acting as a blockade to the migration of the oil throughout the field. The porosity in the field exists as micro-porosity and the thicker oil may not be able to travel through the smaller pores. This would trap not only the heavy oil, but also the light oil, in compartments across the field.

6.1.2 Distinction of Oils by Functional Groups

The separate oil types were divided based on their apparent visual gravities before being analyzed by FT-IR to determine if these gravity variations were due to different organic compounds. Based on the resulting spectra, the samples can be split into two distinct groups (Figure 22), confirming the distinction of the oils into two groups based upon physical characteristics. The FT-IR results show that all of the light oil samples have very similar spectra and can be grouped together. This is also apparent when analyzing the spectra of the heavy oil samples. The spectra of the light oils differ from the heavy; the heavy oils have a greater number of peaks present across their spectra.

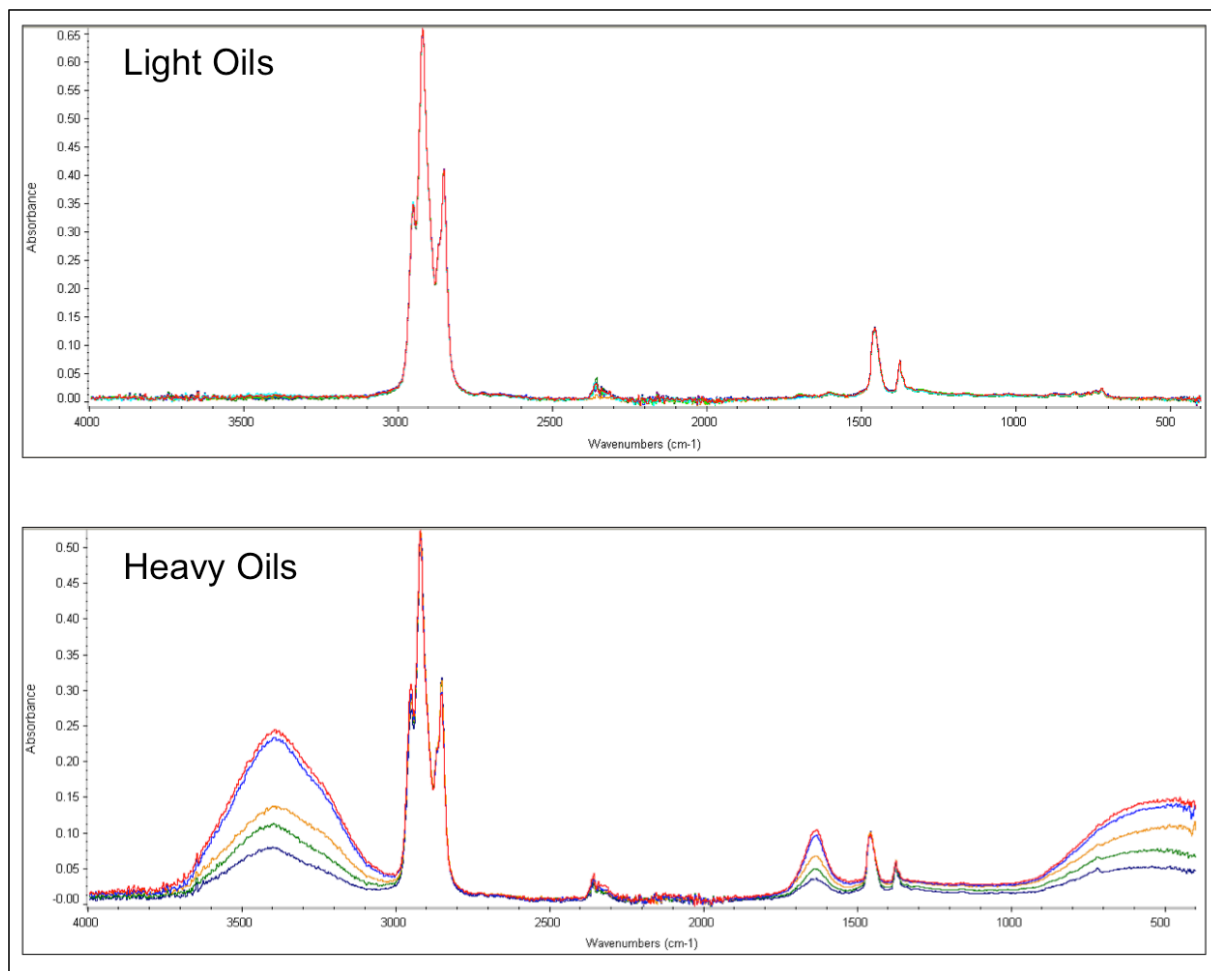


Figure 22. FT-IR spectra of crude oil samples from the Spivey-Grabs field showing two distinct groups. Top) all light oil spectra; bottom) all heavy oil spectra.

It is clear that the oils that appear to be heavier in nature are indeed distinctly different from those that appear to be lighter. Figure 23 highlights peaks that are present in the spectra of the heavy oils, but absent in those of the light. The peak located between the frequencies of 3700 cm^{-1} and 3100 cm^{-1} indicates the presence of O-H stretching bonds in the heavy oil, suggesting that these contain higher quantities of aromatics. The peak located between 1700 cm^{-1} and 1600 cm^{-1} represents C=C stretching of aromatic rings. The absorbance of these frequencies in all of the heavy oils and none of the light oils is evidence that there are two chemically different oils in the Spivey-Grabs field.

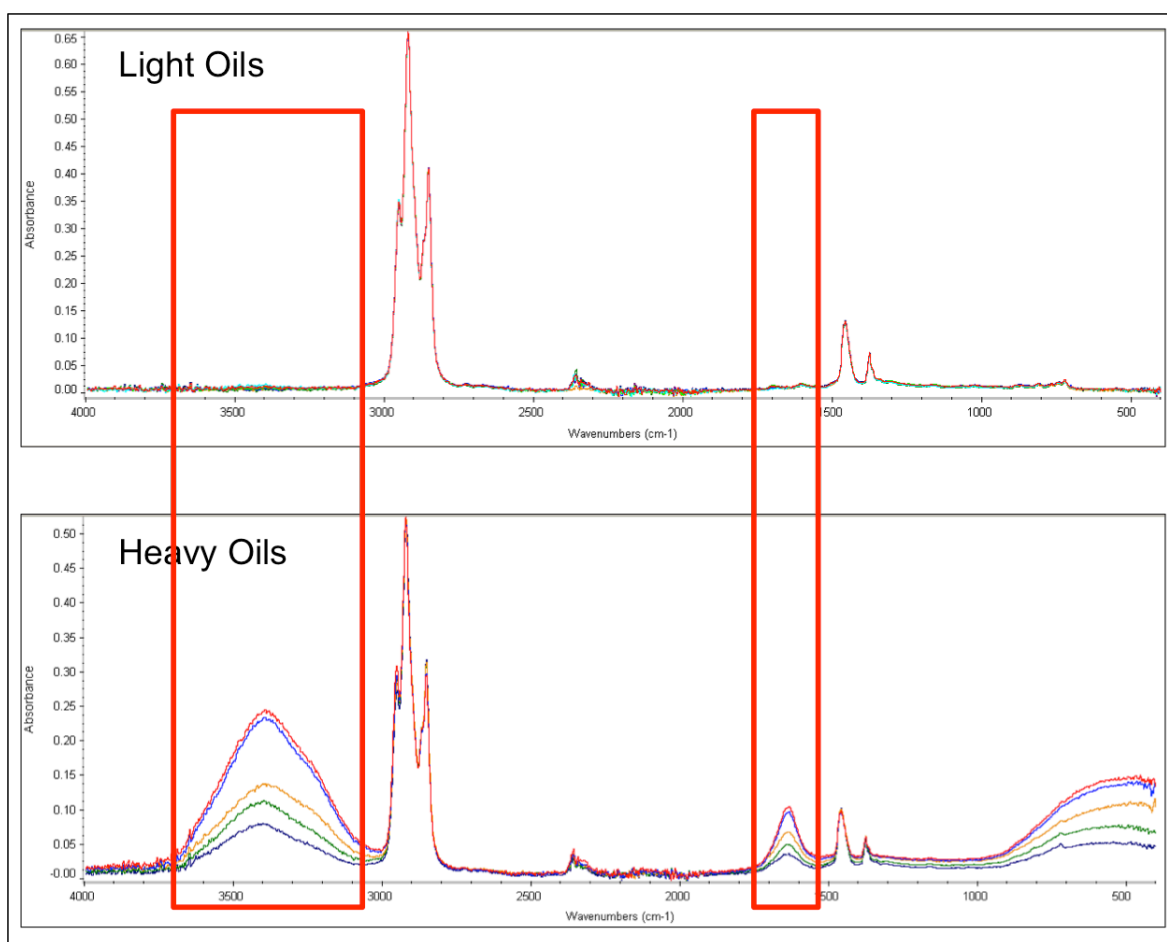


Figure 23. FT-IR spectra of light and heavy oils highlighting peaks that are present in the heavy oil but not in the light oil.

The difference in the first derivatives of two samples, one light and one heavy, from a single well shows that the oils differ greatly. Figure 24 shows that the change in slope between samples BK-14-09A and BK-14-09B occurs at different intensities and at different frequencies along the spectrum. A variation in the spectra of two samples indicates that they have different chemical structures.

The difference between the first derivatives shown from 3000 cm^{-1} to 2800 cm^{-1} , the spectral range that provides information on C-H alkanes, shows that there is a shift in the location of the peaks; the peaks in the spectrum of BK-14-09A are shifted closer to the frequency range of CH_3 asymmetric stretching than BK-14-09B. This peak shift suggests that BK-14-09A has more CH_3 bonds than BK-14-09B. The increased amount of CH_3 bonds in BK-14-09A implies that it has shorter chain lengths than BK-14-09B, further supporting the observation that BK-14-09B is a heavier oil. This relationship is present between all oil samples, providing further evidence that two types of oil are present in the Spivey-Grabs field.

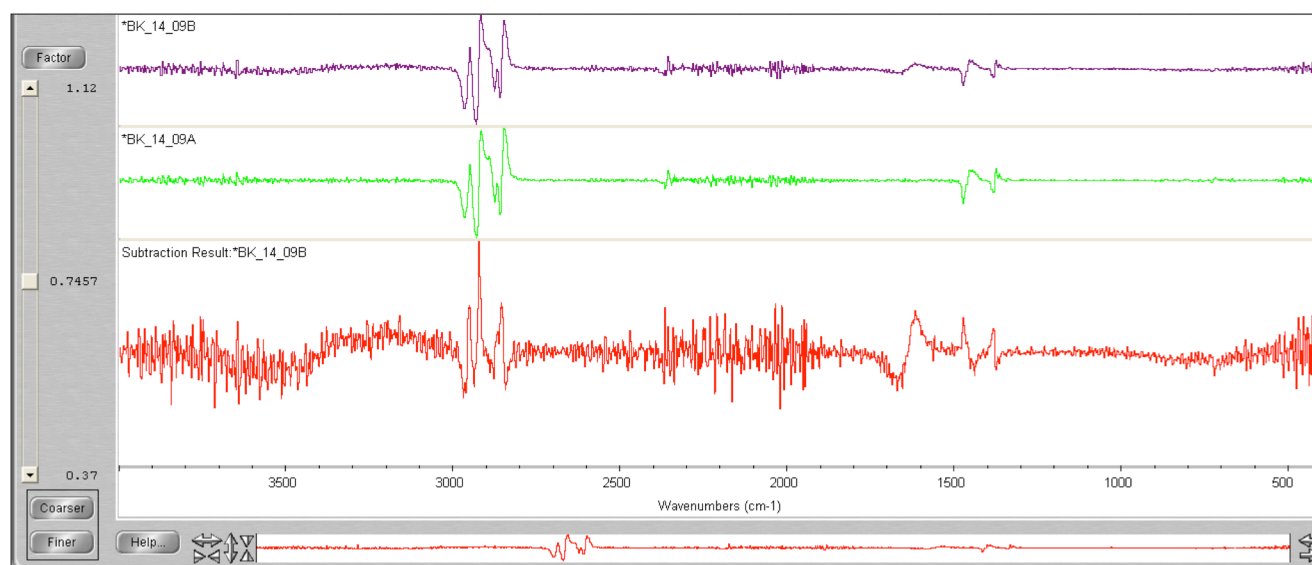


Figure 24. Graph showing the first derivatives of both BK-14-09A and BK-14-09B, as well as the difference in their first derivatives. This shows that there is a peak shift located between 2800 cm^{-1} and 3000 cm^{-1} .

6.2 Field Compartmentalization Due to Two Different Oils Within the Field

The 2011 study completed by Evans found no evidence of the observed “compartmentalization” in the field resulting from lithological barriers or structural features, based upon the distribution of wells with different biomarkers. It is a distinct possibility that the behavior of the field is actually caused by the presence of two separate and distinct oils within the same reservoir. As stated above, the physical characteristics and FT-IR results suggest the field contains a light oil and a heavy oil. The lighter oil would be more easily produced, due to its lower viscosity and lack of water held by the heavier oil. Each well appears to have a different proportion of these two components, which would affect the production rates of that well. These differences in production rates may have been inaccurately ascribed to “compartmentalization”.

It is not clear from these results, however, whether the two different types of oil, heavy versus light, could have migrated from a single source at two different times, or from two distinct organic source rocks. It is also possible that the oils were degraded into two oils after migration into the reservoir rocks. Evans (2011) discussed this possibility.

6.3 Distribution of Rare Earth Elements in Spivey-Grabs Oil

Total rare earth element concentrations in crude oils from the Spivey-Grabs field show values from 2.00×10^{-2} ppb to 1.37×10^{-1} ppb. This compares to values from previous studies of 6.60×10^{-2} ppb to 1.44×10^{-1} ppb in Mississippian oils from the Anadarko basin, 1.50×10^{-2} to 1.19×10^{-1} ppb for Woodford oils, and 3.20×10^{-3} to 1.31×10^{-1} ppb for Lansing-Kansas City oils in western Kansas. The REE distribution patterns of the oil from the Spivey-Grabs, normalized to the Post Achaean Australian Shale (PAAS) are shown in Figure 25. There is a general LREE

enrichment with a MREE and HREE depletion in most samples. Three samples show variability in MREE and HREE. The similarity in the enrichment of LREE in all samples may be a reflection of similar genetic origin and could be a signature that can be used for fingerprinting of oils from the Spivey-Grabs field. While all of the samples displayed a LREE enrichment, they differ in their relative distributions of MREE and HREE.

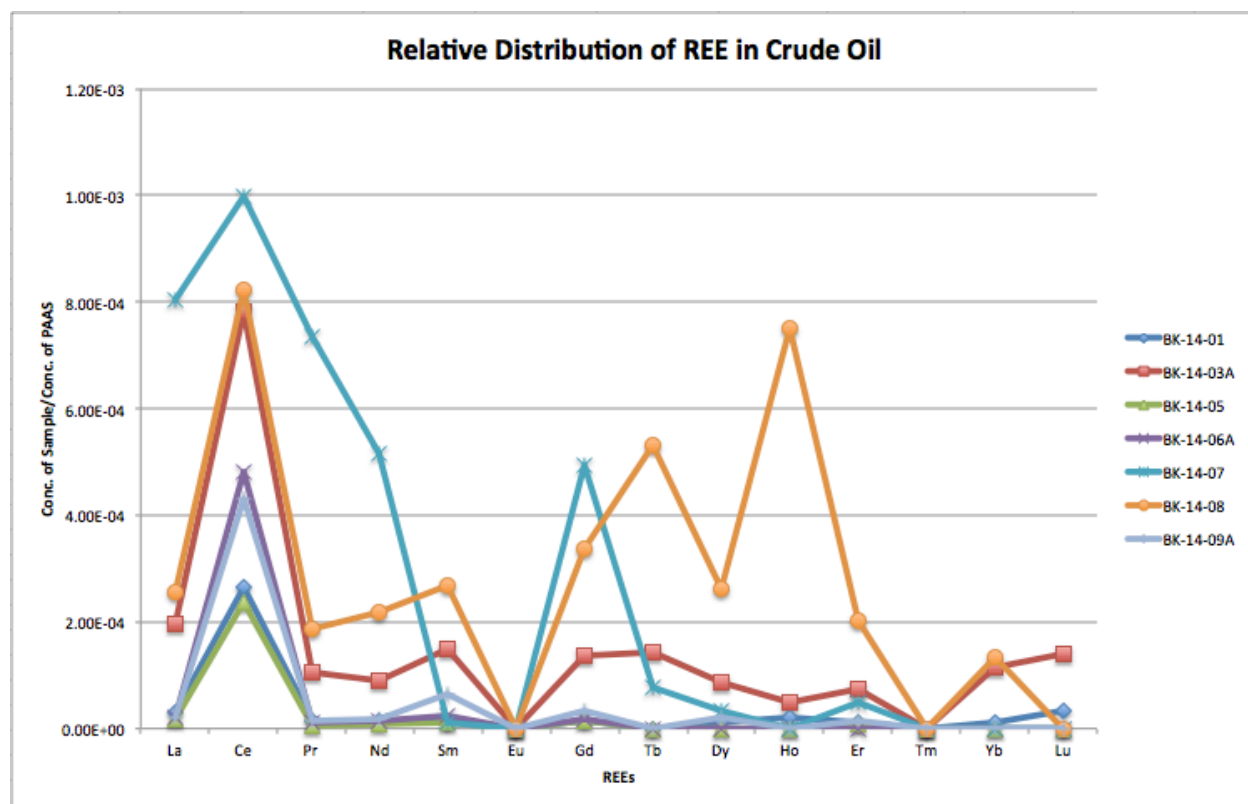


Figure 25. PAAS-normalized abundance diagram displaying the relative distribution patterns of all oil samples from the Spivey-Grabs Field.

6.3.1 REE Anomalies and Similar Distribution Patterns of Spivey-Grabs Crude Oil

Several oil samples show positive cerium anomalies and negative europium anomalies (Figure 25). The variable value of the calculated positive cerium anomaly (Table 5) could be a reflection of the parent material of the oils, as many of the organic matter precursors often show

a negative anomaly, as seen in Figure 26. The cerium is preferentially incorporated into the oils, leaving a deficiency in the organic matter. The anomaly is more positive in the oils than it is negative in the organics left behind because the volume of organic matter greatly exceeds the volume of oil produced.

Sample	Ce/Ce*
BK-14-01	12.1043036
BK-14-03A	5.2230221
BK-14-05	19.6201671
BK-14-06A	30.6795287
BK-14-07	1.29819999
BK-14-08	3.73082643
BK-14-09A	24.9565043

**Table 5. Extent of cerium anomaly in each sample.
Samples also in Evans (2011) are highlighted in blue.**

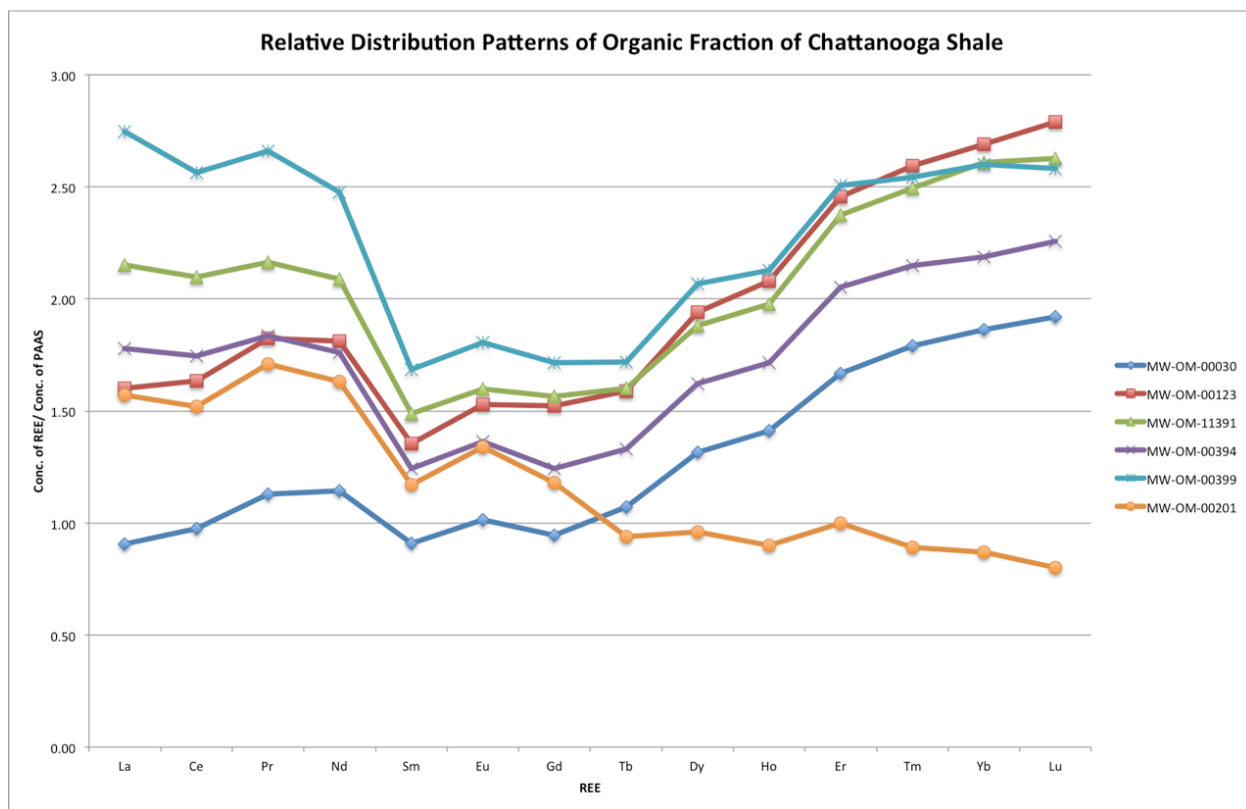


Figure 26. REE distribution patterns of organic portion of the Chattanooga shale showing negative Ce anomalies and positive Eu anomalies (Wall, 2015).

While a positive Ce anomaly and a negative Eu anomaly are present in all Spivey-Grabs samples, the concentrations of the other REEs vary. The samples can be grouped by their relative distribution patterns into three distinct groups. Samples BK-14-01, BK-14-05, BK-14-06A, and BK-14-09A all have similar relative distribution patterns (Figure 27). These samples display an enrichment in LREEs and a general depletion in MREEs and HREEs.

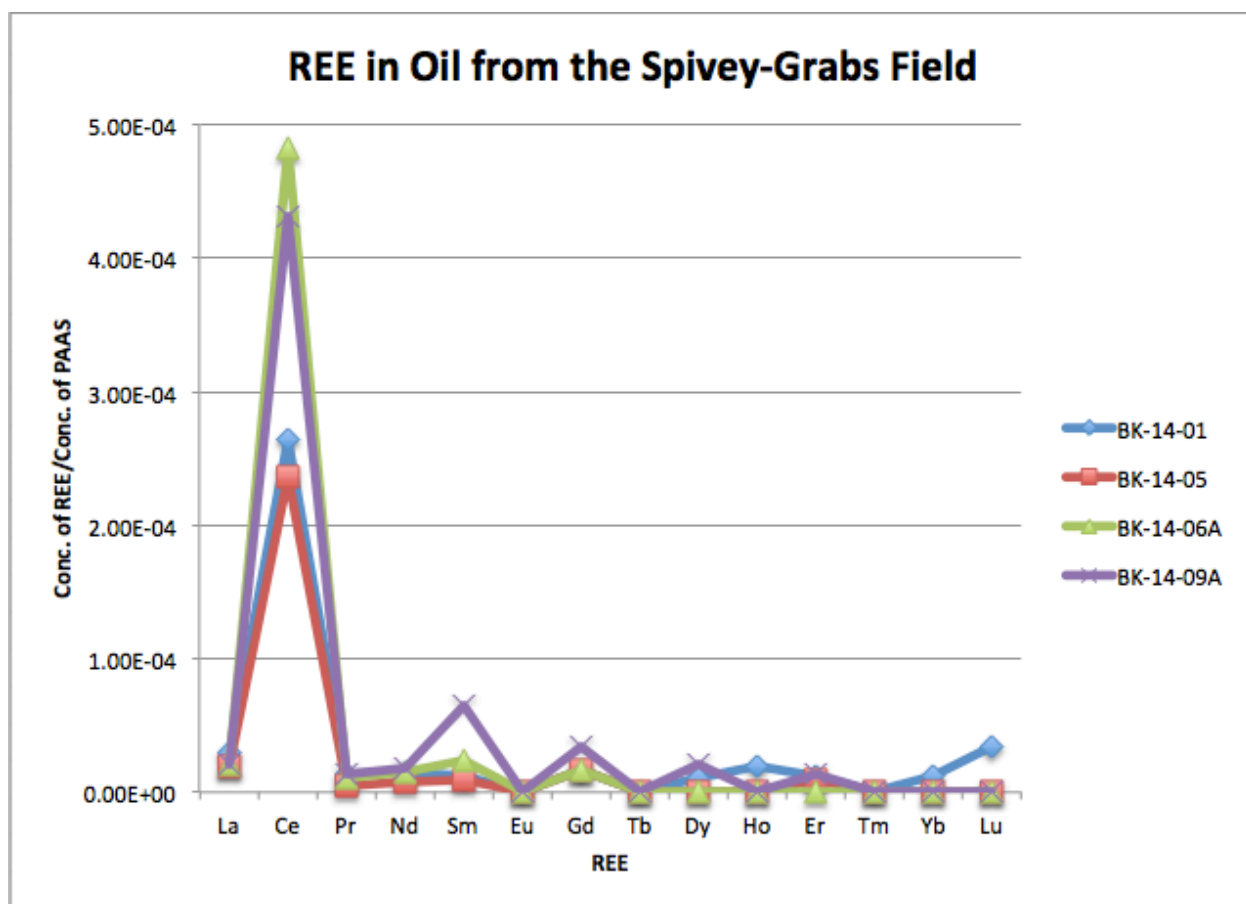


Figure 27. Relative distribution patterns of REEs grouped by similar distribution patterns.

Samples BK-14-03A, BK-14-07 and BK-14-08 cannot be grouped with the four aforementioned samples. Their distribution patterns are distinct from the others. The distribution patterns of BK-14-03A and BK-14-07 show an enrichment in LREEs and MREEs and a general decrease in HREE (Figure 28) while the distribution pattern of BK-14-08 shows an overall “zig-zag” pattern across all of the REEs, LREE, MREE, and HREE (Figure 29).

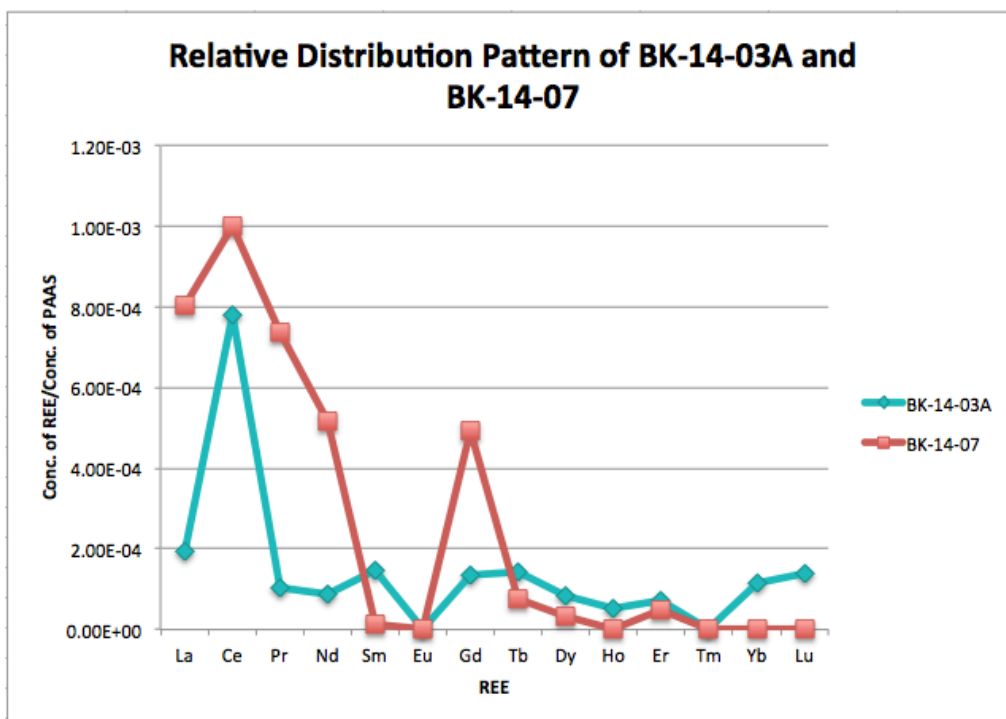


Figure 28. Relative distribution pattern of REEs in BK-14-03A and BK-14-07 grouped by similar distribution patterns.

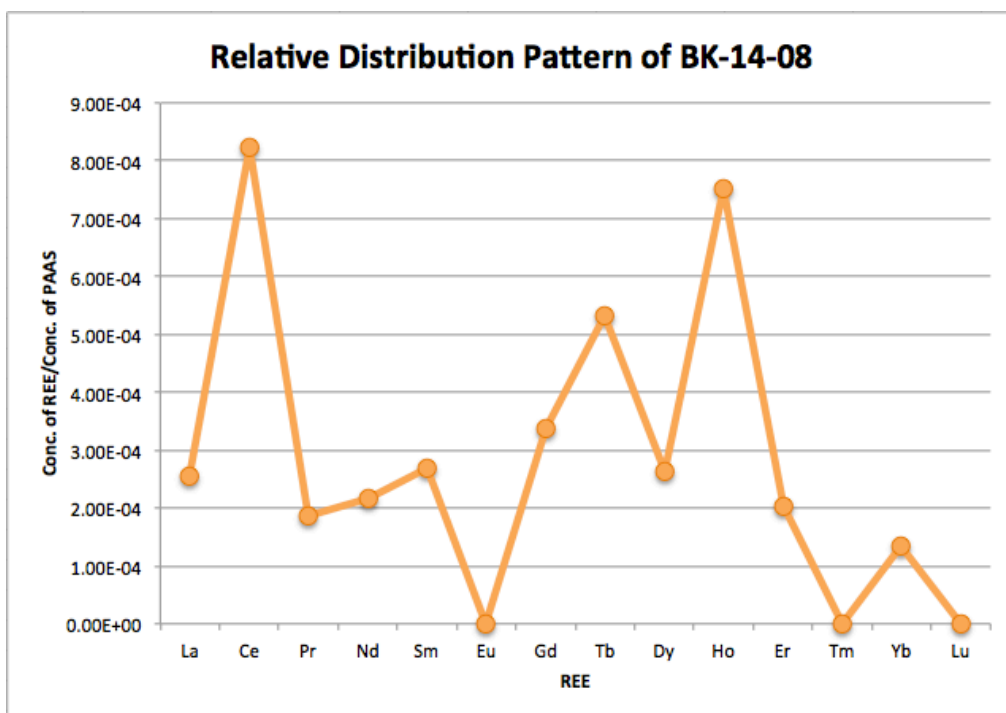


Figure 29. Relative distribution pattern of REEs in BK-14-08.

The absence of HREEs in samples BK-14-01, BK-14-03A, BK-14-05, and BK-14-09A could have been caused by the absence of carboxyl groups in the crude oil (R. Nakada et al., 2010) while post depositional phenomena effects of REE-carbonate complexes or REE-carboxyl complexes may have caused the enrichment of HREE in BK-14-08 because the stability constants of the REE-carbonate complexes and the REE-carboxylic complexes have been found to increase progressively with increasing atomic number (Ramirez-Caro et al., 2013). The general enrichment in MREE in BK-14-03A and BK-14-07 could be attributed to higher concentrations of available phosphorous during organic matter transformation increasing the concentration of the phosphates in the oil.

Samples BK-14-03A, BK-14-07, and BK-14-08 have varying prominently anomalous relative distributions for elements such as Gd, Tb, Ho and Tm. Positive and negative anomalies for these elements imply potential biogenic enzyme influence. The positive Ho anomaly found in BK-14-08 has been common with Eu and Ce in natural materials. This Ho anomaly, as well as the Gd, Tb, and Tm anomalies could be reflections of the growth history of the organic source material. Their different relative distributions may have resulted from enzymatic influences that arose during the growth of the organic materials.

Overall variations in REE distribution patterns could be due to variations in the type of porphyrins in the oils. Metal-porphyrin complexes contain different types of metals in differing amounts. These porphyrins are mainly associated with the asphaltic portion of petroleum (Dunning and Moore, 1957), and therefore, the asphaltenes carry signatures of porphyrins. The heavier oils contain greater amounts of asphaltenes, causing them to have increased metal concentrations and varieties. This could explain the presence of MREEs and HREEs in BK-14-08.

In summary, the REE relative distribution patterns of the crude oils from the Spivey-Grabs field appear to give insight into their origins. While the LREE enrichment in all seven of the samples suggests a similar genetic origin, the different anomalies seen throughout the samples implies differing input sources of the material that generated those anomalies. This implies that the oil probably either originated from two similar sources with slightly different parent material, that the oils originated from a single source, but were expelled from the source during separate pulsing events with different maturation levels, or that the oil originated from different locations within a single source, leading the oil to have higher concentrations of specific REEs in one location than another (A. Akinlua et al., 2008; Chaudhuri, 2014).

6.3.2 REE Distribution Patterns of Spivey-Grabs Crude Oil Compared to Other Oils

The relative distribution patterns of the crude oils from the Spivey-Grabs field can be compared to those from the Lansing-Kansas City formation and the Mississippian and Woodford shale oils from the Anadarko basin when all REE concentrations are normalized to the same constant. The REE concentrations in all three studies were PAAS-normalized before being analyzed.

The oils from the Lansing-Kansas City formation were divided into four groups based on their REE relative distribution patterns (Figure 15). Samples BK-14-01, BK-14-05, BK-14-06A and BK-14-09A from this study are very similar to MM-WM-11A, MM-MC-1A, and MM-MC-4A from McIntire 2014. As shown in Figure 30, all seven of these samples have a LREE enrichment with a general depletion in MREE and HREE. The similarities in their distribution patterns suggest that the oils have a similar genesis. The remaining crude oil sample from the

Spivey-Grabs field, BK-14-07, cannot be easily grouped with any of the distribution patterns from the Lansing-Kansas City formation.

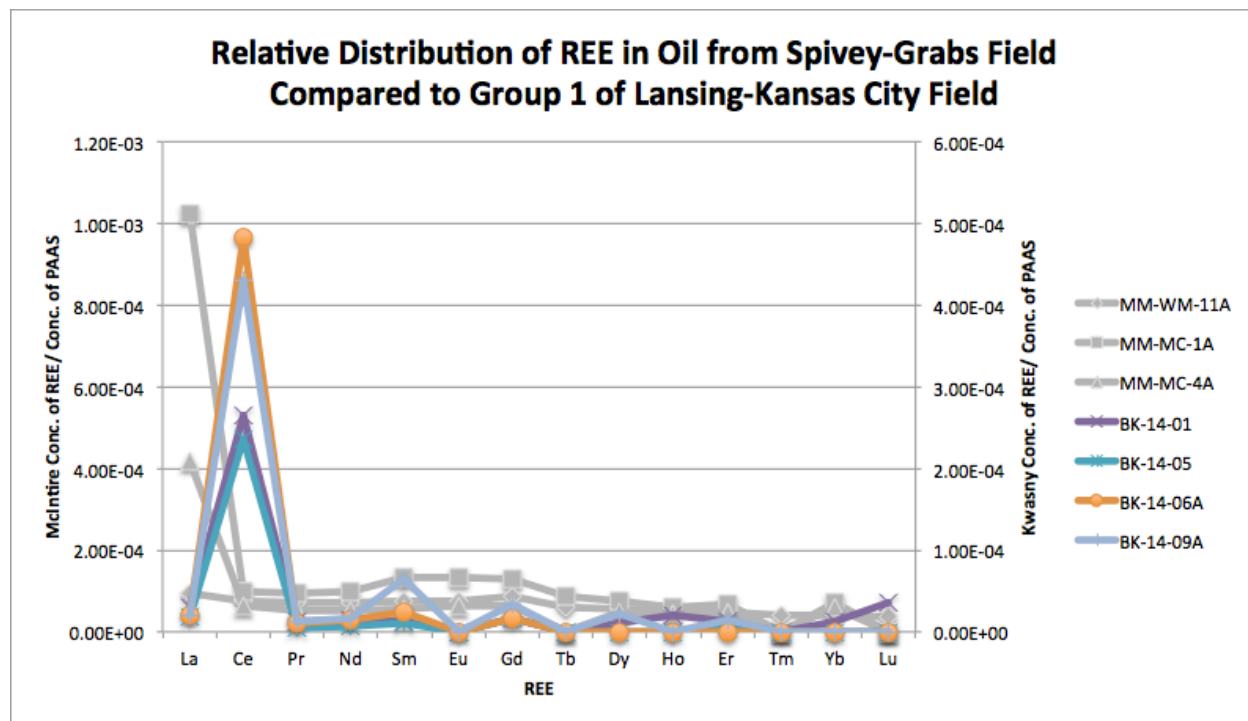


Figure 30. Relative distribution patterns of REE in crude oils samples from the Spivey-Grabs field and McIntire's (2014) Lansing-Kansas City samples grouped by similar distribution patterns. All seven samples have an enrichment of LREE and depletion of MREE and HREE.

In his 2013 study, Ramirez-Caro found that the relative distribution patterns of his samples from both the Woodford shale and the over-lying Mississippian had a general enrichment in LREE and a strong positive Eu anomaly (Figure 17). Many of the samples, five out of the seven Mississippian samples and three out of the six Woodford shale samples, showed a negative cerium anomaly. While the general LREE enrichment for these samples is also present in the relative distribution patterns of the Spivey-Grabs crude oil, the positive Eu anomaly and negative Ce anomaly are opposite of them. Ramirez-Caro's samples also show, overall, a much higher

distribution of all LREE, MREE, and HREE. Because the REE distribution patterns of these oils are so different, it can be inferred that they did not originate from the same source.

6.4 Trace Metals Indicate Two Oil Types and Local Source

Total trace metal concentrations varied between the samples. However, results from ICP-AES (Table 4) showed that the heavier samples BK-14-03B, BK-14-04, BK-14-06B, BK-14-08, and BK-14-10 had higher concentrations overall. These samples were all higher viscosity oils. This is further evidence of two types of oil in the field.

6.4.1 K/Rb Values of the Spivey Grabs Field Oil

The K/Rb values of the crude oil samples from the Spivey-Grabs field range from 2,864 to 44,118 with an average of approximately 18,320 (Figure 31). According to Chaudhuri (2014) and Chaudhuri et al. (2007), silicate minerals, like feldspar and mica, have a K/Rb value ranging from 50 to 650 while the K/Rb values of organics, such as plants, are most commonly 300 – 10,000, but can reach upwards of 50,000. Crude oil samples BK-14-01, BK-14-05 and BK-14-07 all have K/Rb values greater than 18,000. Each of these samples originated from a well with only light oil collected. Samples BK-14-03A, BK-14-06A, and BK-14-08, all collected from wells with mixed-gravity oils (both light and heavy oil), have K/Rb ratios between 2800 and 11,000. BK-14-09A has a K/Rb of 24,138. The decreased K/Rb values in the mixed-gravity crude oils could be resulting from K/Rb exchange between the light and heavy oils, with the heavy oils decreasing the concentration of potassium in the light oils. Apart from BK-14-09A, the light oils and the mixed-gravity oils can be separated into two distinct groups, providing further evidence for the presence of two types of oil in the field.

The wide variability in K/Rb values shows that when K and Rb are studied in conjunction with each other, the K/Rb ratio can be a strong geochemical tracer for the source of K in a system. Comparing K/Rb values found in crude oils to known K/Rb values of other materials can provide information on the source and migration history of the oils (S. Chaudhuri et al., 2007 and Chaudhuri, 2014).

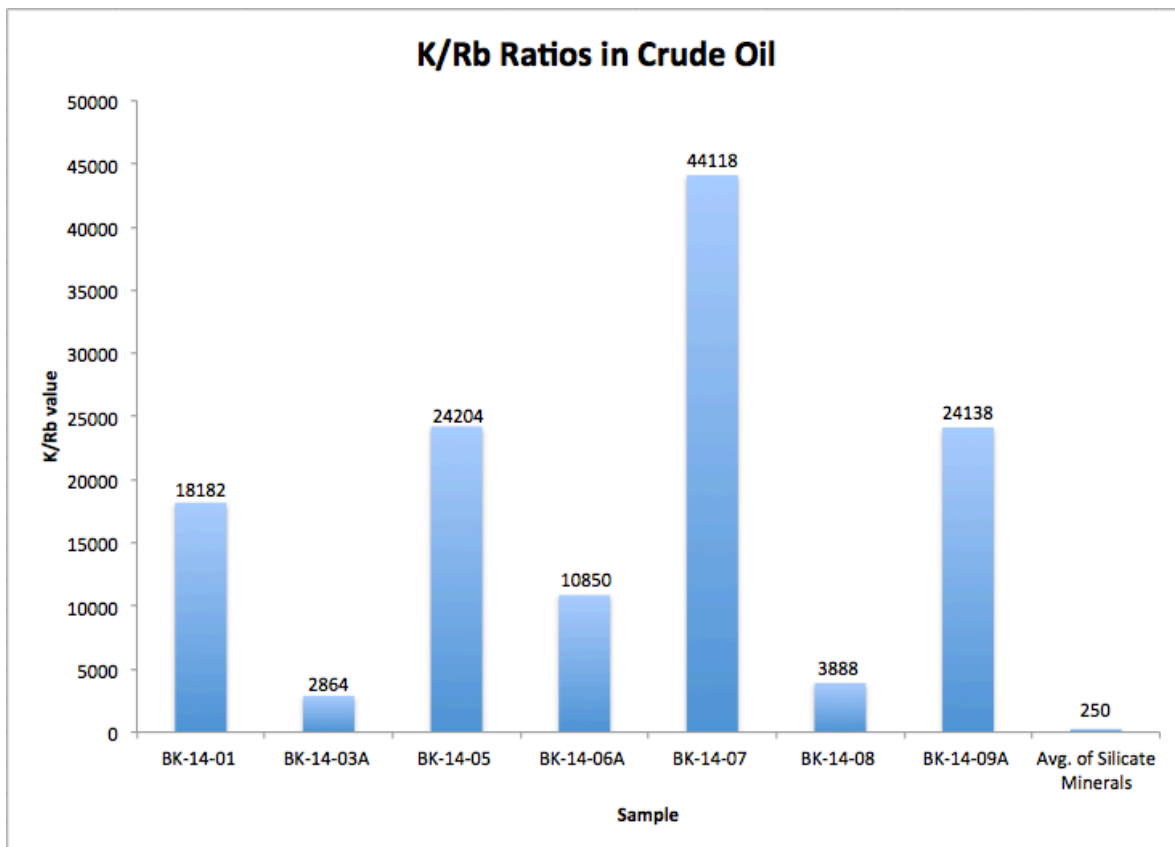


Figure 31. Chart showing the K/Rb values of crude oils from the Spivey-Grabs field compared to the average K/Rb value of silicate minerals/clays.

Potassium is transferred to waters through two pathways: the weathering of silicate minerals and the decay of plant and biomass material that releases some of the K the plants accumulated to surface and ground waters (S. Chaudhuri et al., 2007). According to P. Peltola et al. (2008), Potassium and Rubidium are important to study when analyzing the origin of hydrocarbons because K is essential for all forms of life and is taken up by plants in its cationic

form (K^+) and Rb, while having no biological function, is often affected by the concentration of K. The availability of K in soils affects Rb because the uptake of Rb is sensitive to changes in soil; when there are sufficient concentrations of K in soil, lower levels of Rb are absorbed by the soil. This results in typically higher K/Rb ratios in biological materials than in soils and silicate or carbonate rocks.

The high values of these crude oils indicate that the K concentrations were sourced from plant material and not solely from surrounding rocks. According to Chaudhuri (2014), the values also suggest that the oils did not migrate far from the source in two ways: 1) the values are relatively high compared to those of silicate minerals found in rocks. If the oils had travelled far from the source, they would have picked up metals, such as Rb, from the rocks they migrated through, thus decreasing the K/Rb values; 2) there is a high level of variance between the sample values. Oils that migrate long distances are expected to have exchanged K/Rb values with the rocks they migrated through and therefore have more uniform values. Because this is not the case with the Spivey-Grabs oils, it can be inferred that the oils probably did not migrate far from their source.

6.4.2 K/Rb Values of Spivey Grabs Oil Compared to Other Oils

The K/Rb values of crude oils from the Spivey-Grabs field, although overall much higher, fall in the same range as the crude oils McIntire found in his 2014 study of crude oil from the Lansing-Kansas City formation (Figure 32). The Lansing-Kansas City oil has K/Rb ratios that range from 877 to 2000 with an average of 1110. K/Rb values from both fields fall in the range of those defined as organics. This suggests that the oils from both fields could share a similar genesis. Both the Spivey-Grabs oil and the Lansing-Kansas city oil have K/Rb values that are much higher than those found in Ramirez-Caro's 2013 study of the Woodford and Mississippian

oils from the Anadarko basin. The K/Rb ratios from the Anadarko basin oils fall within the range of the values for silicate mineral, 50 to 650. The much lower K/Rb values of the Mississippian and Woodford crude oils of the Anadarko basin compared to those of the Lansing-Kansas City formation and the Spivey-Grabs field suggest that the Mississippian and Woodford oils are sourced from a different origin.

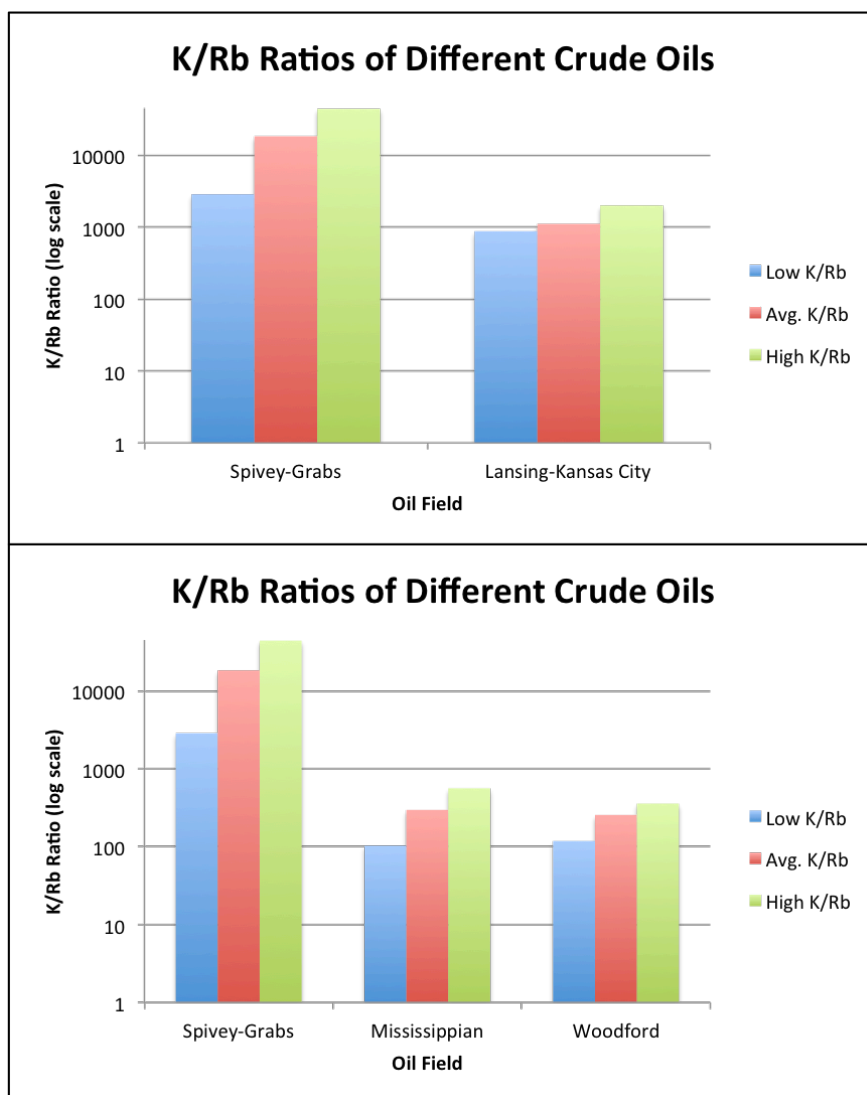


Figure 32. High, low, and average K/Rb ratios from crude oils from: Top) the Spivey-Grabs field and Lansing-Kansas City formation; Bottom) the Spivey Grabs field and the Mississippian and Woodford oils from the Anadarko basin. Compared on a logarithmic scale.

6.5 Biomarker Maturation Groups Compared to Inorganic Constituents

This study did not result in a correlation between the inorganic constituents in the Spivey-Grabs crude oil and the two biomarker maturation index groups (Table 6) found in Evans' (2011) study of the organic constituents. This could potentially be due in part to the fact that trace metal distributions in crude oil seem not to be affected by maturation (A. Akinlua et al., 2015), and trace metal ratios in crude oils remain unchanged irrespective of diagenetic and in-reservoir alteration affects (A. Akinlua et al., 2007). A second potential reason for the absence of correlation between the results is that, according to Chaudhuri (2015), a correlation between the biomarker maturation indices and the metals of the oils, including the REE distribution patterns and K/Rb values, may not exist because trace metal concentrations can provide information on variations within a single type of organic matter which could be too detailed to compare to analysis of the organic constituents. However, ICP-MS results for samples BK-14-03B, BK-14-04, BK-14-06B, and BK-14-10 would give more complete results and could provide more information on REEs and K/Rb, leading to a better understanding, and potentially a correlation.

This study separated some of the samples that contained both light and heavy oils and analyzed them individually, while Evans (2011) analyzed all the oil from each well without separating it. This study found that there are two oils in the field based on viscosity and FT-IR. As thermal maturation increases, an oil's API gravity increases and viscosity decreases (Peters et al., 2005; Peters et al., 2012). The oil samples used in this study were allowed to sit long enough that they separated by specific gravity into different viscosities, showing what could be oils of two different maturities, and as a result, they were analyzed separately. However, the two groups of oils found in this study did not correlate to the two biomarker maturation index groups Evans' determined. This lack of correlation between the samples could potentially be a result of the

different methods used to analyze the samples. The correlation may have existed if: 1) The samples in this study were not separated before analyzing or 2) Evans' samples had sat long enough to separate and had been analyzed based on viscosity.

Table 6. Inorganic constituent analyses compared to biomarker maturation indices from Evans (2011). Blue) less mature oil group; red) mature oil group; white) not analyzed in Evans' study.

Well	Sample	Oil in Well	REE Pattern	Ce/Ce*	K/Rb
Bruch No. 1	BK-14-01	Light	LREE	12.1	18182
Pound No. 1	BK-14-03A	Mixed	LREE	5.22	2864
Maple G No. 1	BK-14-05	Light	LREE	19.6	24204
Maple F No. 1	BK-14-06A	Mixed	LREE	30.7	10850
Maple F No. 2	BK-14-07	Light	LREE, MREE	1.3	44118
Krehbiel B No. 1	BK-14-08	Mixed	LREE, MREE, HREE	3.73	3888
Coykendall No. 10	BK-14-09A	Mixed	LREE	24.96	24138

6.6 Implications of REE Distribution Pattern and K/Rb Comparisons

Crude oils in mid-Continent reservoirs have been thought to have migrated north from a primary source of the Woodford shale in central Oklahoma by many previous authors (see summary in Hill, 2011). If the oils were indeed sourced from the Woodford shale, the oils would have had to travel hundreds of miles to reach central Kansas reservoirs. Some geologists believe that the oil in Kansas actually originated from a local source, and not the Woodford shale. McIntire's 2014 study of crude oils from the Lansing-Kansas City formation used REE distributions patterns and K/Rb to show that the geochemistry of the oil suggested it originated from a local source. The REE distribution patterns and K/Rb ratios for the crude oil from the Spivey-Grabs field suggest that it also originated from a local source. The REE distribution patterns differ greatly from those of oil from the Anadarko basin, but are very similar to crude oil

samples from the Lansing-Kansas City formation. The high K/Rb values suggest influence from organic material and not surrounding rocks, while the large variance between samples indicates a small amount of interaction and trace element exchange between the oil and rocks during migration. The K/Rb ratios of the crude oil of both the Spivey-Grabs field and the Lansing-Kansas City formation suggest that their values were more highly influenced by organic matter/plant material than from silicate minerals. This implies that they likely did not migrate far from their sources. All of this suggests that the Kansas oils originated from a more proximal source.

Chapter 7 - Conclusions

Results from the geochemical analysis of the inorganic constituents and infrared spectroscopy of the crude oils from the Spivey-Grabs field of south-central Kansas suggest the following:

1. Physical characteristics suggest there are two different types of crude oil in the field, heavy and light. This is supported by FT-IR results showing C-H alkane peak shifts between the two types indicating the presence of CH_3 in type one (light) and longer CH_2 chains in type two (heavy), along with the presence of water and aromatics in higher viscosity oil but not lighter oil.
2. The presence of such heavy oil could be the cause of the compartmentalization in the field. The heavy oil could be acting as a trap, clogging areas with micro-pores that are too small for it migrate through and keeping the lighter oil from moving through the pores as well.
3. REE relative distribution patterns display a general LREE enrichment, a positive Ce anomaly and a negative Eu anomaly in all samples. This suggests a similar genetic origin for all samples.
4. When compared to those from the Lansing-Kansas City formation (McIntire, 2014) and the Mississippian and Woodford shale of the Anadarko basin (Ramirez-Caro, 2013), the REE relative distribution patterns of Spivey-Grabs crude oils most closely resemble the oils from the Lansing-Kansas City formation, suggesting that these two oils have a similar source.
5. K/Rb ratios of crude oils from the Spivey-Grabs field range from 573 to 8824. These values fall in the range of K/Rb values for organics (300 – 10,000) and not silicate minerals (50 – 650). This suggests they were influenced by organics and not surrounding rocks, signifying a local origin. The high variance in K/Rb ratios is indicative of a local

source; if the oils had migrated from a distant source, they would have travelled through many different rocks, altering their K/Rb values to match those of silicate minerals instead of those of their parent material. The K/Rb ratios more closely match those of McIntire's 2014 study of the Lansing-Kansas City formation than those of Ramirez-Caro's 2013 study of the Mississippian and Woodford shale of the Anadarko basin. This implies that the oils from the Spivey-Grabs field and the Lansing-Kansas City formation have a similar source that differs from that of the Mississippian and Woodford shale oils.

The combined results and conclusions from this analysis suggest that REE and trace metal concentrations of the oils in the Spivey-Grabs Field that, in addition to biomarkers, provide information and understanding on the source and history of crude oil. The similarities found between all the oils in the field also suggest that the inorganic constituents can be used as an additional way to type oil.

References

- Abanda, P.A. and Hannigan, R.E., 2006. Effect of diagenesis on trace element partitioning in shales: *Chemical Geology*, Vol. 230, pp. 42-59.
- Akinlua, A., Ajayi, T. R., Adeleke, B. B., 2007. Organic and inorganic geochemistry of northwestern Niger Delta oils: *Geochemical Journal*, Vol. 41, pp.271-281.
- Akinlua, A., Torto, N., and Ajayi, T.R., 2008. Determination of rare earth elements in Niger Delta crude oils by inductively coupled plasma-mass spectrometry: *Fuel*, Vol. 87, pp. 1469-1477.
- Akinlua, A., Sigedle, A., Buthelezi, T., and Fadipe, O.A., 2015. Trace element geochemistry of crude oils and condensates from South African basins: *Marine and Petroleum Geology*, Vol. 59, pp. 286-293.
- Berthomieu, C. and Hienerwadel, R., 2009. Fourier transform infrared (FTIR) spectroscopy: *Photosynthesis Research*, Vol. 101, No. 2, pp. 157-170.
- Chaudhuri, S., Clauer, N., and Semhi, K., 2007. Plant decay as a major control of river dissolved potassium: A first estimate: *Chemical Geology*, Vol. 243, pp. 178-190.
- Chaudhuri, S., 2014. Personal Communication.
- Chaudhuri, S., 2015. Personal Communication.
- Cotton, F.A. and Wilkinson, G., 1962. *Advanced Inorganic Chemistry*: Interscience Publishers, John Wiley and Sons, New York – London.
- Dao-Hui, P., Cong-Qiang, L., Shields-Zhou, Graham A., and Shao-Youn, J., 2013. Trace and rare earth element geochemistry of black shale and kerogen in the early Cambrian Niutitang Formation in Guizhou province, South China: Constraints for redox environments and origin of metals: *Precambrian Research*, Vol. 225, pp. 218-229.
- Dunning, H.N. and Moore, J.W., 1957. Porphyrin research and origin of petroleum: *American Association of Petroleum Geologists Bulletin*, Vol. 40, No. 11, pp. 2403-2412.
- Ege, S., 1989. "Infrared Spectroscopy." *Organic Chemistry*, 2nd ed. Lexington: D.C. Heath. Pp. 355-75.
- Evans, C.H., 1990. *Biochemistry of Lanthanides*. New York: Plenum Press.
- Evans, C.H. and Newell, D.K., 2013. The Mississippian limestone play in Kansas: oil and gas in a complex geological setting: *Kansas Geological Survey Public Information Circular No. 33*, 6 p.

- Evans, D., 2011. The compartmentalization and biomarker analysis of the Spivey-Grabs-Basil Field, south-central Kansas. Thesis Dissertation: Kansas State University. 101 p.
- Frensley, R.W. and Darmstetter, J.C., 1965. Spivey-Grans Field. Kansas Geological Survey, 1006 – Kansas Oil and Gas Fields, Vol. 4, pp. 221-228.
- Goebel, E.D., 1971. Southeast Kansas – northeast Oklahoma – southwest Missouri, in Adler, Frank J. et al. Future petroleum provinces of the Mid-Continent. Pp. 1088-1097.
- Harris, R.L. and Larsh, H.A., 1979. Kansas: its geology, economics, and current drilling activity. Oklahoma City Geological Society – The Shale Shaker Digest 9, Vol. 27-29, pp. 326-338.
- Henderson, P., 1984. *Rare Earth Element Geochemistry*. Amsterdam: Elsevier. Print.
- Hill, T.J., 2011. Potential source rocks in the western Kansas petroleum province, Thesis Dissertation: Kansas State University. 88 p.
- Hommertzheim, D., 2014. Personal Communication.
- Hunt, J.M., 1995. *Petroleum Geochemistry and Geology*, 2nd Edition: New York: W. H. Freeman and Company.
- Khuhawar, M.Y., Aslam M.M., and Jahangir, T.M., 2012. Determination of metal ions in crude oils, *Crude Oil Emulsions – Composition Stability and Characterization*. Prof. Manar El-Sayed Abdul-Raouf (Ed.), pp. 121-144.
- Lee, W., 1940. Subsurface Mississippian rocks of Kansas: Kansas Geological Survey Bulletin, Vol. 33, 114 p.
- Lewan, M.D., 1984. Factors controlling the proportionality of vanadium to nickel in crude oils: *Geochemica et Cosmochimica Acta*, Vol. 48, No. 11, pp. 2231-2238.
- Maples, C.G., 1994. Revision of Mississippian stratigraphic nomenclature in Kansas, in D. L. Baars, comp., Revision of stratigraphic nomenclature in Kansas. Kansas Geological Survey Bulletin 230, pp. 67-74.
- Mazzulo, S.J., Wilhite, B.W., and Woolsey, I.W., 2009. Petroleum reservoirs within a spiculite-dominated depositional sequence: Cowley formation (Mississippian: Lower Carboniferous), south-central Kansas. AAPG Bulletin, Vol. 93, No. 12, pp. 1649-1689.
- McIntire, M.C., 2014. Rare earth elements (REE) in crude oil in the Lansing-Kansas City formations in central Kansas: potential indications about their sources, locally derived or long-distance derived. Thesis Dissertation: Kansas State University. 90 p.

- Merriam, D.F., 1963. The geologic history of Kansas. Kansas Geological Survey Bulletin 162. 317 p.
- Montgomery, S.L., Mullarkey, J.C., Longman, W.M., and Rogers, J.P., 1998. Mississippian “Chat” reservoirs, south Kansas: low resistivity pay in a complex chert reservoir. AAPG Bulletin, Vol. 82, No. 2, pp.187-205.
- Nakada, R., Takahashi, Y., Zheng, G., Yamamoto, Y., and Shimizu, H., 2010. Abundances of rare earth elements in crude oils and their partitions in water: Geochemical Journal, Vol. 44, pp. 411-418.
- Peltola, P., Brun, C., Åström, M., and Tomilina, O., 2008. High K/Rb ratios in stream waters – Exploring plant litter decay, ground water, and lithology as potential controlling mechanisms: Chemical Geology, Vol. 257, pp. 92-100.
- Peters, K.E., Valters, C.C., and Moldowan, M.J., 2005. *The Biomarker Guide: Biomarkers and in the Environment and Human History*: Cambridge University Press, 1155 p. Print.
- Peters, K.E., Curry, D.J., and Kacwicz, M., 2012. *Basin Modeling: New Horizons in Research and Applications*: AAPG Hedberg Series, No. 4, 338 p.
- Ramirez-Caro, D., 2013. Rare earth elements (REE) as geochemical clues to reconstruct hydrocarbon generation history. Thesis Dissertation: Kansas State University. 103 p.
- Ramirez-Caro, D., Totten, M., Chaudhuri, S., Clauer, N., Boutin, R., Miesse, J., Riepl, G., Semhi, K., 2013. Rare earth elements (REE) as transformation indicators of organic matter; case study of the Woodford shale, North Central Oklahoma; Unconventional Reservoir Technology Conference, 11 p.
- Rogers, J.P., Longman, M. W., Lloyd, R. M., 1996. Spiculitic chert reservoir in Glick Field, south-central Kansas. Tulsa Geological Society: Transactions of the 1995 AAPG Mid-Continent Section Meeting, 1996. 31 p.
- Rogers, J.P. and Longman, M.W., 2001. An introduction to chert reservoirs of North America. AAPG Bulletin, Vol. 85, No. 1, pp.1-5.
- Scotese, C.R., 1999. Paleomap Project Website: <<http://www.scotese.com/>>.
- Smith, F.G., 1963. *Physical Geochemistry*: Addison-Wesley Publishing Company, Reading, Massachusetts, 624 p.
- Soin, A., Maryutina, T., Musina, N., and Soin, A., 2012. New possibility for REE determination in oil: International Journal of Spectroscopy, Vol. 2012, 5 pp.

- Wall, M., 2015, An oil-source rock correlation examining the potential of the Chattanooga shale as a source rock for oil within the Spivey-Grabs-Basil field, Kingman and Harper Counties, Kansas, Thesis Dissertation: Kansas State University, 79 p.
- Watney, W.L., Guy, W.J., and Byrnes, A.P., 2001. Characterization of the Mississippian chat in south-central Kansas. AAPG Bulletin, Vol. 85, No. 1, pp. 85-113.
- Witzke, B.J., 1990. Paleoclimatic constraints for Paleozoic paleolatitudes of Laurentia and Euramerica, in W.S. McKerrow and C. R. Scotese, eds., Paleozoic paleogeography and biogeography: London, Geological Society Memoir 12, pp. 57-73.
- Zeller, D.E., Jewett, J.M., Bayne, C.K., Goebel, E.D., O'Conner, H.G., and Swineford, A., 1968. The stratigraphic succession in Kansas. Kansas Geological Survey Bulletin 189. 81 p.

Appendix A - Rare Earth Elements (REE)

The Lanthanide elements (Ln) or Rare Earth Elements (REEs) are a group of 14 elements ranging from lanthanum (La) to lutetium (Lu). These elements range in atomic number from 57 to 71 (Figure A.1) and are located in block 5d of the periodic table. REEs are the first elements to fill the f-orbitals, having completely filled the $5s^2$, $4d^{10}$, $5p^6$, and $6s^2$ orbitals. The REEs have differing electronic configurations based on the energy orbitals beyond $6s^2$ that their electrons fill (4f orbitals or 5d orbital). All of the REEs exist as trivalent ions (Ln^{3+}) except for europium (Eu) and cerium (Ce); europium also occurs as a divalent ion (Eu^{2+}) and cerium also occurs with a valence of 4 (Ce^{4+}).

Periodic Table of the Elements

																		18 VIIIA 8A														
1 1A H Hydrogen 1.008																	2 He Helium 4.003															
3 Li Lithium 6.941	4 Be Beryllium 9.012																	5 B Boron 10.811	6 C Carbon 12.011	7 N Nitrogen 14.007	8 O Oxygen 15.999	9 F Fluorine 18.998	10 Ne Neon 20.180									
11 Na Sodium 22.990	12 Mg Magnesium 24.305																	13 Al Aluminum 26.982	14 Si Silicon 28.086	15 P Phosphorus 30.974	16 S Sulfur 32.06	17 Cl Chlorine 35.45	18 Ar Argon 39.948									
19 K Potassium 39.098	20 Ca Calcium 40.078	21 Sc Scandium 44.956	22 Ti Titanium 47.88	23 V Vanadium 50.942	24 Cr Chromium 51.996	25 Mn Manganese 54.938	26 Fe Iron 55.845	27 Co Cobalt 58.933	28 Ni Nickel 58.693	29 Cu Copper 63.546	30 Zn Zinc 65.38	31 Ga Gallium 69.723	32 Ge Germanium 72.64	33 As Arsenic 74.922	34 Se Selenium 78.96	35 Br Bromine 79.904	36 Kr Krypton 83.8															
37 Rb Rubidium 85.468	38 Sr Strontium 87.62	39 Y Yttrium 88.906	40 Zr Zirconium 91.224	41 Nb Niobium 92.906	42 Mo Molybdenum 95.94	43 Tc Technetium 98.906	44 Ru Ruthenium 101.07	45 Rh Rhodium 102.905	46 Pd Palladium 106.42	47 Ag Silver 107.868	48 Cd Cadmium 112.411	49 In Indium 114.818	50 Sn Tin 118.71	51 Sb Antimony 121.757	52 Te Tellurium 127.6	53 I Iodine 126.905	54 Xe Xenon 131.29															
55 Cs Cesium 132.905	56 Ba Barium 137.327	89-103		72 Hf Hafnium 178.49	73 Ta Tantalum 180.948	74 W Tungsten 183.84	75 Re Rhenium 186.207	76 Os Osmium 190.23	77 Ir Iridium 192.22	78 Pt Platinum 195.08	79 Au Gold 196.967	80 Hg Mercury 200.59	81 Tl Thallium 204.383	82 Pb Lead 207.2	83 Bi Bismuth 208.980	84 Po Polonium 209	85 At Astatine 210	86 Rn Radon 222														
87 Fr Francium 223	88 Ra Radium 226	89-103		104 Rf Rutherfordium 261	105 Db Dubnium 262	106 Sg Seaborgium 266	107 Bh Bohrium 264	108 Hs Hassium 277	109 Mt Meitnerium 268	110 Ds Darmstadtium 271	111 Rg Roentgenium 272	112 Cn Copernicium 285	113 Nh Nihonium 284	114 Fl Flerovium 289	115 Uup Ununpentium 288	116 Lv Livermorium 293	117 Uus Ununseptium 289	118 Uuo Ununoctium 294														
																		57 La Lanthanum 138.905	58 Ce Cerium 140.12	59 Pr Praseodymium 140.908	60 Nd Neodymium 144.24	61 Pm Promethium 144.913	62 Sm Samarium 150.36	63 Eu Europium 151.964	64 Gd Gadolinium 157.25	65 Tb Terbium 158.925	66 Dy Dysprosium 162.50	67 Ho Holmium 164.930	68 Er Erbium 167.26	69 Tm Thulium 168.934	70 Yb Ytterbium 173.04	71 Lu Lutetium 174.967
																		89 Ac Actinium 227.028	90 Th Thorium 232.038	91 Pa Protactinium 231.036	92 U Uranium 238.029	93 Np Neptunium 237.048	94 Pu Plutonium 244.064	95 Am Americium 243.061	96 Cm Curium 247.07	97 Bk Berkelium 247.07	98 Cf Californium 251.08	99 Es Einsteinium 252	100 Fm Fermium 257.10	101 Md Mendelevium 258.10	102 No Nobelium 259.10	103 Lr Lawrencium 262

Atomic Number

Valence Charge

Symbol

Name

Atomic Mass

Lanthanide Series

Actinide Series

© 2013 Todd Helmenstein

chemistry.about.com

helmenstein.org

Figure A.1. Rare earth elements (lanthanide series) in the Periodic Table of Elements.

A main property of the REEs that make them excellent tracers for defining many different natural organic and inorganic geological processes is the “lanthanide contraction.” The lanthanide contraction is the progressive reduction in atom size (or ionic radius) with increasing atomic number (Table A.1) (Smith, 1963; Evans, 1990). As the atomic number of the REE increases, there is an increasing insufficient shielding of the increasing nuclear attractive force with each additional proton in the nucleus and the accompanying additional electron that fills the 4f orbital (Cotton and Wilkinson, 1962). As a result of this insufficient shielding and resultant reduction in size of the entire 4f subshell, the lanthanide contraction arises.

Table A.1. Atomic number and ionic radii for the REE

Element	La	Ce	Pr	Nd	Pm	Sm	Eu	Gd	Tb	Dy	Ho	Er	Tm	Yb	Lu
Atomic electron configuration (all begin with [Xe])	5d ¹ 6s ²	4f ¹ 5d ¹ 6s ²	4f ³ 6s ²	4f ⁴ 6s ²	4f ⁵ 6s ²	4f ⁶ 6s ²	4f ⁷ 6s ²	4f ⁷ 5d ¹ 6s ²	4f ⁹ 6s ²	4f ¹⁰ 6s ²	4f ¹¹ 6s ²	4f ¹² 6s ²	4f ¹³ 6s ²	4f ¹⁴ 6s ²	4f ¹⁴ 5d ¹ 6s ²
Atomic number	57	58	59	60	61	62	63	64	65	66	67	68	69	70	71
Ln ³⁺ radius (pm) (6coordinate)	103.2	101	99	98.3	97	95.8	94.7	93.5	92.3	91.2	90.1	89	88	86.8	86.1

The REEs have very similar chemical properties because differences between them exist primarily in the 4f orbitals that their electrons fill. As a result of having such similar characteristics, REE changes in chemistry are hard to study. REEs often exist in materials as a group and have obvious distribution patterns. However, not all REEs respond to stimulation from chemical changes in natural materials in the same way; therefore, the relative distribution

patterns of REEs are studied (Chaudhuri, 2014). The REEs have been subdivided into three groups based on which ones commonly occur together (Figure A.2):

1. Light REEs: La, Ce, Pr, Nd, Sm, and Eu (atomic number 57 to 63)
2. Middle REEs: Sm, Eu, Gd, Tb, Dy, and Ho (atomic number 62 to 67)
3. Heavy REEs: Gd, Tb, Dy, Ho, Er, Tm, Yb, Lu (atomic number 64 to 71)

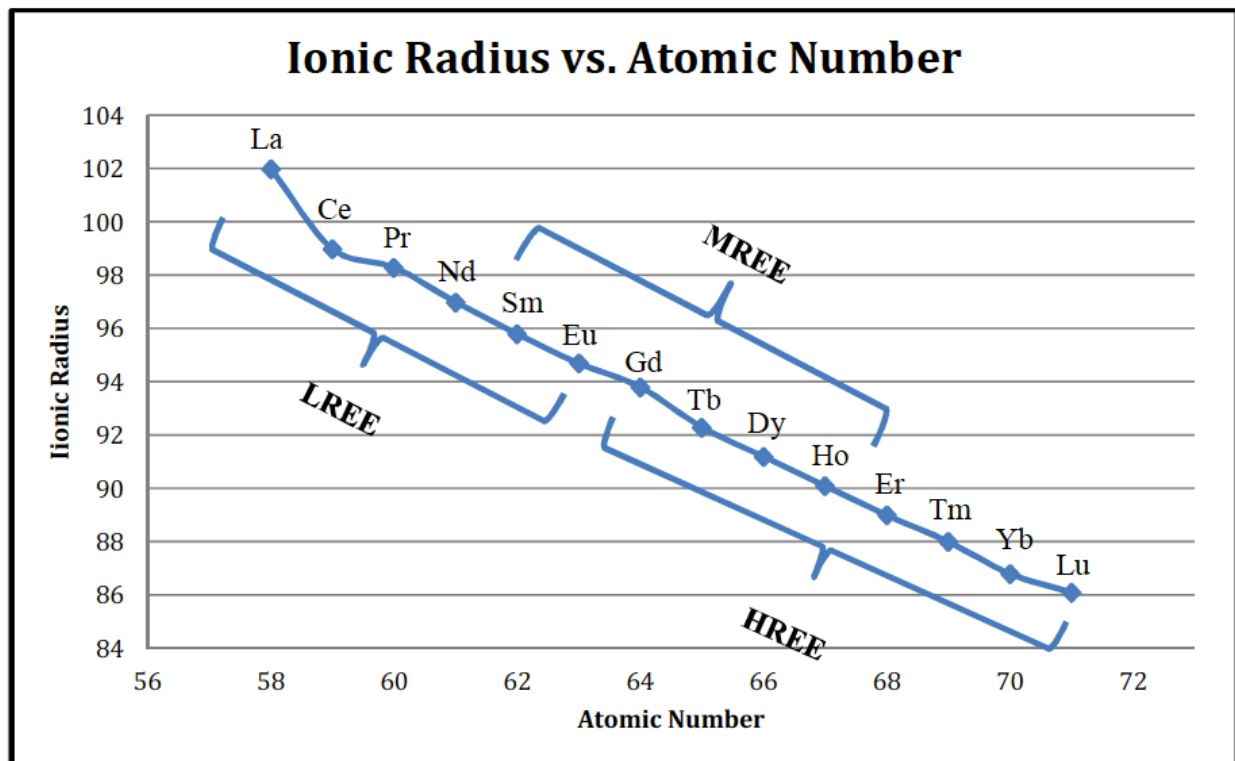


Figure A.2. Graph depicting lanthanide contraction and REE relative distribution pattern groups.

Appendix B - REE Distribution Patterns

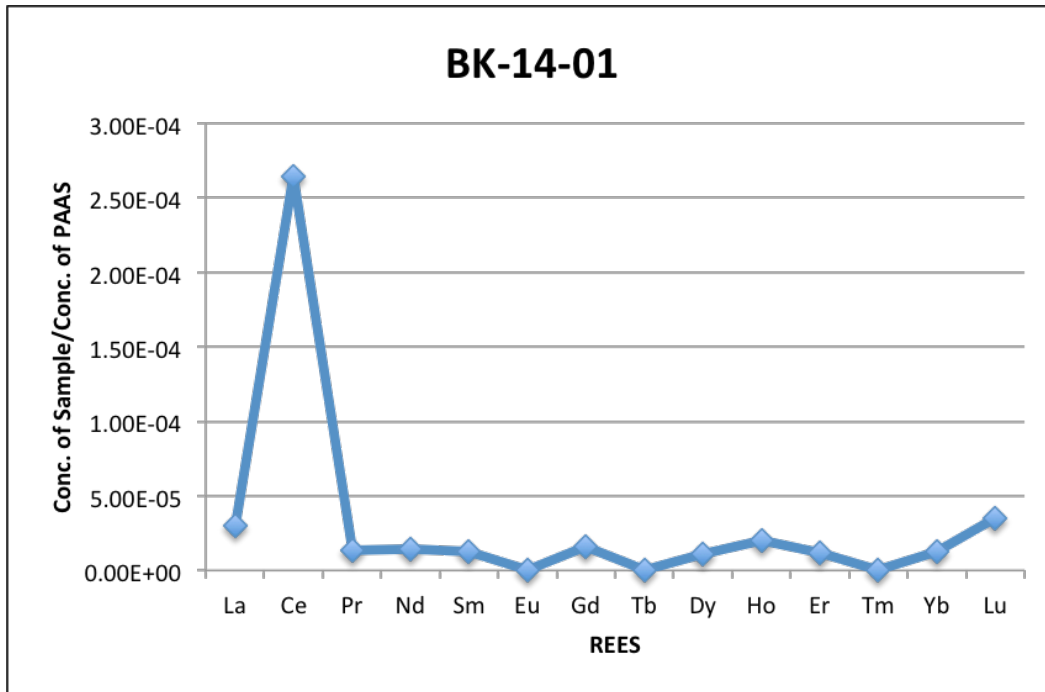


Figure B.1. REE distribution pattern of BK-14-01.

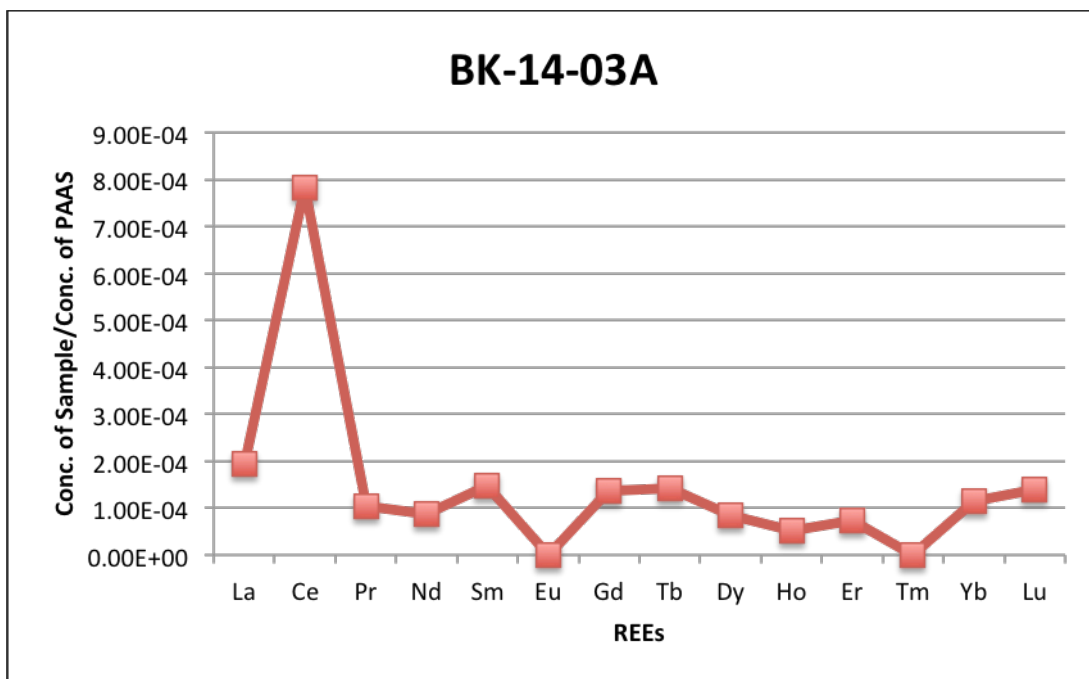


Figure B.2. REE distribution pattern of BK-14-03A.

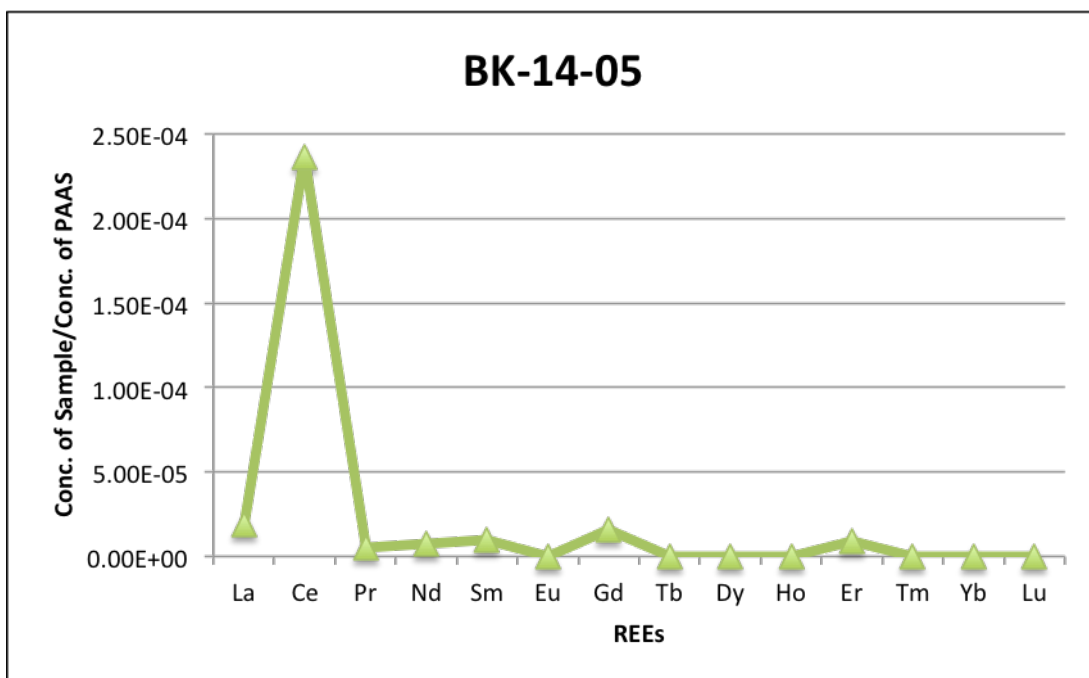


Figure B.3. REE distribution pattern of BK-14-05.

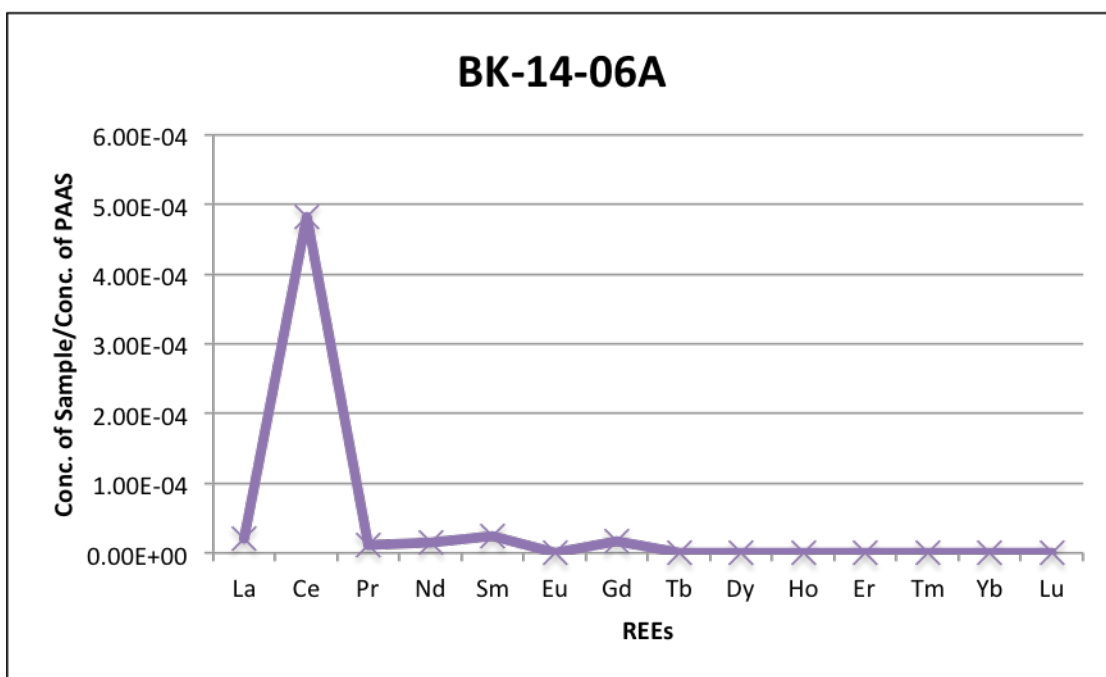


Figure B.4. REE distribution pattern of BK-14-06A.

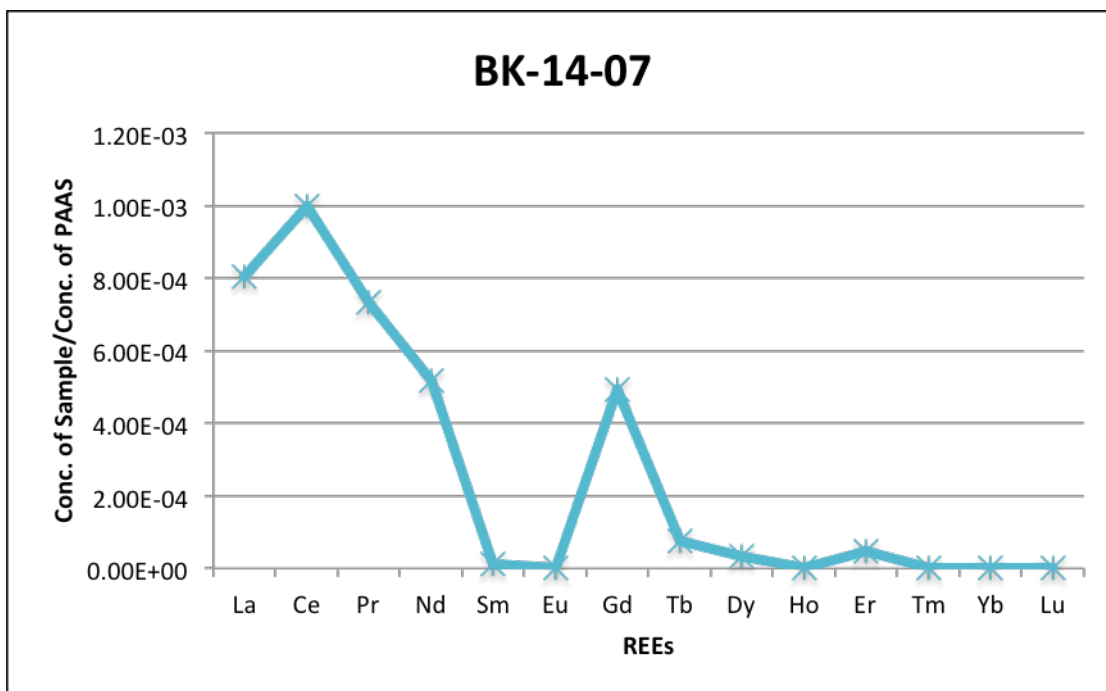


Figure B.5. REE distribution Pattern of BK-14-07.

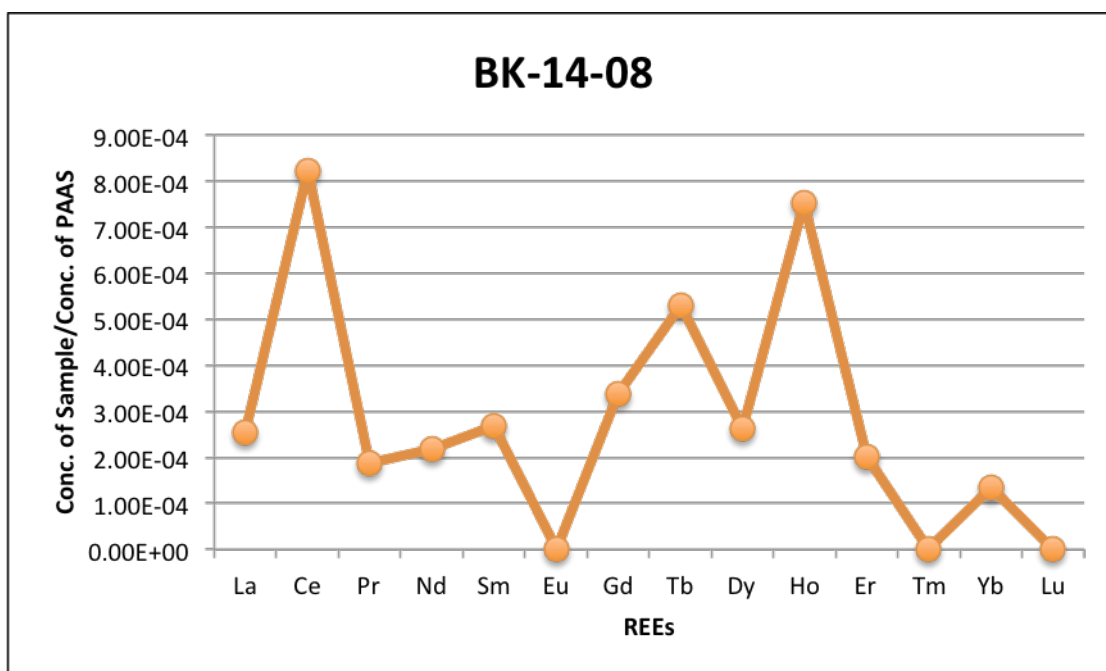


Figure B.6. REE distribution pattern of BK-14-08.

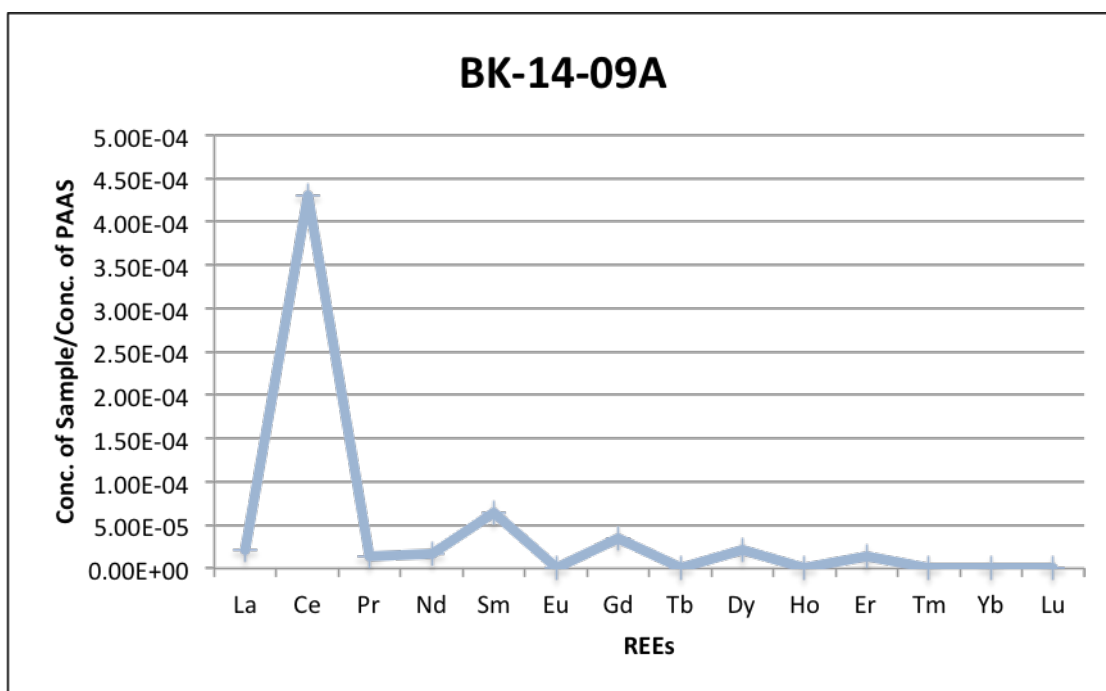


Figure B.7. REE distribution pattern of BK-14-09A.

Appendix C - Fourier Transform Infrared Spectroscopy (FT-IR)

Spectrophotometers are instruments that monitor the absorption of the energy of a molecule resulting from its transition between fixed energy levels (ground states and excited states) when it interacts with electromagnetic radiation. Spectrophotometers record the changing absorption of energy as a function of the wavelength or the frequency of the radiation being used.

The chemical bonds of a molecule are distorted by the constant motion of the atoms within the molecule. These vibrations either cause a change in bond length, known as stretching vibrations, or a change in bond angles, known as bending vibrations (Berthomieu and Hienerwadel, 2009 and Ege, 1989). According to Seyhan Ege (1989), there are multiple energy levels for any given molecule that each have specific spacings. The energy levels correspond to different vibrational states that are possible for each molecule and the spacings correspond to the energy of radiation in the infrared region of the electromagnetic spectrum. If a change in the dipole moment of the molecule occurs during vibration, the vibration is “infra-red active” (Berthomieu and Hienerwadel, 2009), meaning that the infrared radiation is absorbed by the molecule. This absorption usually occurs at a frequency between 4000 and 600 cm^{-1} . The instrument that records the absorption of infrared radiation as a tracing is known as an infrared spectrophotometer.

The recorded tracing that results from absorbed infrared radiation results in a spectrum that is recorded by a Fourier-Transform Infrared Spectrophotometer (FT-IR spectra). While an infrared spectrum is generated by the molecule as a whole, absorption peaks within the spectrum correspond to the frequencies of bond vibrations between the atoms that make up that molecule. Each compound produces a peak unique unto itself; therefore, infrared spectra can be used to

identify the specific materials within the molecule. This means that functional groups, such as the carbonyl group or the hydroxyl group, can be identified by their characteristic infrared absorption bands (Table B.1) (Berthomieu and Hienerwadel, 2009 and Ege, 1989). By studying the FT-IR spectra of oil samples, one can determine which functional groups make up that oil.

Table C.1. Table showing the assignment of the primary infrared bands/peaks to functional groups.

Frequency (cm⁻¹)	Definition of the Spectral Assignments
3400 cm ⁻¹	O-H alcohols and water stretching bands
2930 - 2860 cm ⁻¹	CH stretching bands of alkyl groups
1710 cm ⁻¹	C=O stretching band
1630 cm ⁻¹	C=C stretching of aromatic and polyaromatic rings
1450 cm ⁻¹	Peptidic amide band
1455 cm ⁻¹	Asymmetric bending of CH ₂ and CH ₃ groups
1375 cm ⁻¹	Mainly due to symmetric bending of CH ₃ groups
870-750 cm ⁻¹	out of the plane of deformation of aromatic CH groups
720 cm ⁻¹	Sharp band due to skeletal vibration of straight chains with more than 4 CH ₂ groups

Appendix D - Sample Dilutions

Table D.1. Sample dilutions that occurred during preparation of the samples for analysis.

SAMPLE	ORIGINAL VOL.	AR ADDED	H2O ADDED	TOTAL ADDED	PRE-FILTERED	POST-FILTERED VOL.	FINAL SOLN.
BK-14-01	1000 mL	15 mL	60 mL	75 mL	45 mL	43 mL	5 mL
BK-14-02	1000 mL	20 mL	10 mL	30 mL	15 mL	12 mL	10 mL
BK-14-03A	1000 mL	15 mL	30 mL	45 mL	29 mL	22 mL	10 mL
BK-14-03B	420 mL	15 mL	40 mL	55 mL	42 mL	17 mL	10 mL
BK-14-04	475 mL	15 mL	20 mL	35 mL	32 mL	20 mL	10 mL
BK-14-05	1000 mL	15 mL	55 mL	70 mL	39 mL	35 mL	5 mL
BK-14-06A	1025 mL	15 mL	45 mL	60 mL	48 mL	36 mL	10 mL
BK-14-06B	375 mL	15 mL	20 mL	35 mL	32 mL	22 mL	10 mL
BK-14-07	1000 mL	15 mL	45 mL	60 mL	36 mL	28 mL	10 mL
BK-14-08	900 mL	15 mL	45 mL	60 mL	40 mL	34 mL	10 mL
BK-14-09A	1000 mL	15 mL	50 mL	65 mL	40 mL	38 mL	10 mL
BK-14-10	450 mL	15 mL	15 mL	30 mL	25 mL	22 mL	10 mL